



CHALMERS
UNIVERSITY OF TECHNOLOGY



Driver subjective feedback study during crosswind gusts on driving simulator for high speed straight line driving

Master's thesis in Automotive Engineering

ANUP GARJE MOHANKUMAR
SAI KISHAN SAWANTH

DEPARTMENT OF MECHANICS AND MARITIME SCIENCES

CHALMERS UNIVERSITY OF TECHNOLOGY

Gothenburg, Sweden 2022

www.chalmers.se

MASTER'S THESIS IN AUTOMOTIVE ENGINEERING

Driver subjective feedback study during crosswind gusts on driving simulator for high speed straight line driving

ANUP GARJE MOHANKUMAR
SAI KISHAN SAWANTH



CHALMERS
UNIVERSITY OF TECHNOLOGY

Department of Mechanics and Maritime Sciences
Vehicle Engineering and Autonomous Systems
CHALMERS UNIVERSITY OF TECHNOLOGY
Gothenburg, Sweden 2022

Driver subjective feedback study during crosswind gusts on driving simulator for high speed straight line driving

ANUP GARJE MOHANKUMAR
SAI KISHAN SAWANTH

© ANUP GARJE MOHANKUMAR 2022.
© SAI KISHAN SAWANTH 2022.

Master's Thesis 2022:62
Department of Mechanics and Maritime Sciences
Vehicle Engineering and Autonomous Systems
Chalmers University of Technology
SE-412 96 Gothenburg
Telephone +46 (0)31 772 1000

Supervisor: Adam Brandt, Senior Specialist - Industrial PhD, CEVT AB

Examiner: Bengt J H Jacobson, Full Professor in Vehicle Dynamics and leader of Vehicle Dynamics group at Mechanics and Maritime Sciences, Division of Vehicle Engineering and Autonomous Systems, Chalmers University

Cover: Dynamic Driving Simulator at CEVT

Name of the printer: Department of Mechanics and Maritime Sciences Gothenburg, Sweden 2022

Driver subjective feedback study during crosswind gusts on driving simulator for high speed straight line driving

ANUP GARJE MOHANKUMAR
SAI KISHAN SAWANTH
Department of Mechanics and Maritime Sciences
Chalmers University of Technology

Abstract

The passenger vehicle industry develops aerodynamic designs that have low drag to improve vehicle efficiency at high speeds. The low drag aerodynamic design affects crosswind stability during straight line driving, this is crucial for passengers and other road user safety.

The thesis work subjectively evaluates vehicle high-speed stability under crosswind gusts on VI grade DIM 250 moving platform 6 DOF driving simulator. The simulator allowed testing the high speed response of a high-fidelity vehicle model with groups of drivers in a controlled virtual environment. Initial CAE work focuses on the complexity of SUV vehicle models and the implementation of crosswind gusts in the desktop CAE simulation and driving simulator, coupling between aerodynamics and vehicle dynamics. Stochastic crosswind gust tests were designed on Matlab & Simulink and implemented on CarRealTime vehicle dynamics model on the driving simulator that simulated the change in aerodynamic flow conditions and resulting vehicle aerodynamic forces and moments.

Driving clinic is conducted to find the correlation between driver subjective feedback and vehicle's objective metric response. The vehicle crosswind sensitivity is evaluated using a developed proxy measure. Finally, through statistical tests the study found that the subjective instability feeling is triggered by the vehicle change in lateral and centripetal accelerations response amongst the experienced driver and steering torque demand for common drivers during straight line driving at high speeds under aerodynamic crosswind gusts. The implementation of crosswind gusts on driving simulator is evaluated subjectively.

Keywords: aerodynamics, crosswinds, high Speed, driver-in-loop, correlation, objective metrics, subjective assessment, driver sensitivity.

Acknowledgements

We thank our supervisor Adam Brandt for his immense support and guidance during our master thesis work at CEVT (China Euro Vehicle Technology AB). You have given us a wonderful opportunity to develop our knowledge and skills. We express our sincere gratitude to Prof. Bengt Jacobson for giving us a part of his invaluable knowledge through lectures and discussions at Chalmers. We are honored to present our thesis work at the VDCA (Vehicle Dynamics Competence Area) conference held in KTH Royal Institute of Technology and for this we are in debt to Prof. Bengt Jacobson.

A special thanks to Andreas Grip and Eric Gunnarsson for enabling us to conduct a successful driving clinic for two weeks around the clock. The team enjoyed working with you. Our deep appreciation to Jörgen Sjöström, Albin Gröndahl, Martin Ljunggren, Jan Hellberg and Tiago Rocha, you have been very supportive to our study from the very start. You have played an important role in empowering us to improve the driving simulator experience and developing our knowledge in CAE simulation and testing.

The team enjoyed working with the energy team at CEVT and our deepest thanks to Lars Nilsson for giving us an opportunity to work with your team. We extend our warm regards to all our colleagues who participated in the driving clinic and thank you for the supportive feedback. We are in debt to CEVT AB for providing us top notch tools, technology and knowledge.

Last but not least, we wish to thank our family and friends for your patience and support during our thesis work.

ANUP GARJE MOHANKUMAR, Gothenburg, August 2022
SAI KISHAN SAWANTH, Gothenburg, August 2022

Nomenclature

Abbreviations

CAE	Computer-Aided Engineering
CEVT	China-Euro Vehicle Technology
CFD	Computational Fluid Dynamics
CRT	Car Real Time
CWG	Cross Wind Gusts
DIL	Driver-in-the-Loop
DIM	Driver in Motion
DOF	Degrees of Freedom
ISO	International Organization for Standardization
OM	Objective Metrics
SA	Subjective Assessment
ST	Subjective Triggers
SUV	Sport Utility Vehicle

Parameters and variables

A_f	Frontal cross-sectional area	$[m^2]$
C_d	Coefficient of drag force	
C_l	Coefficient of lift force	
C_{pm}	Coefficient of pitch moment	
C_{rm}	Coefficient of roll moment	
C_s	Coefficient of side force	
C_{ym}	Coefficient of yaw moment	
F_d	Aerodynamic drag force	$[N]$
F_{flz}	Front left normal tyre force	$[N]$
$F_{f rz}$	Front right normal tyre force	$[N]$
$F_{f yw}$	Front axle lateral tyre force	$[N]$
F_l	Aerodynamic lift force	$[N]$
F_{rlz}	Rear left normal tyre force	$[N]$
$F_{r rz}$	Rear right normal tyre force	$[N]$
$F_{r yw}$	Rear axle lateral tyre force	$[N]$
F_s	Aerodynamic side force	$[N]$
J_s	Vehicle sprung mass moment of roll inertia	$[kgm^2]$
J_z	Vehicle mass moment of yaw inertia	$[kgm^2]$
K_{fRC}	Front axle roll stiffness	$[N/deg]$
K_{rRC}	Rear axle roll stiffness	$[N/deg]$
M_x	Aerodynamic roll moment	$[Nm]$
M_y	Aerodynamic pitch moment	$[Nm]$
M_z	Aerodynamic yaw moment	$[Nm]$
<i>proxy</i>	Proxy signal measure	
V_{mag}	Relative flow magnitude	$[m/s]$
V_{mag}^f	Relative flow magnitude at front axle	$[m/s]$
V_{mag}^r	Relative flow magnitude at rear axle	$[m/s]$
\vec{a}	Vehicle body acceleration vector	$[m/s^2]$
d_{fRC}	Front axle roll damping	$[Nm/deg/s]$

d_{rRC}	Rear axle roll damping	$[Nm/deg/s]$
h_{fRC}	Front axle roll centre height	$[m]$
h_{rRC}	Rear axle roll centre height	$[m]$
l_f	Distance between COG and front axle	$[m]$
l_r	Distance between COG and rear axle	$[m]$
swa	Steering wheel angle	$[deg]$
$storq$	Steering wheel torque	$[Nm]$
t_0	Gust start time	$[s]$
t_b	Gust build up time	$[s]$
t_d	Gust drop time	$[s]$
t_p	Gust pause time	$[s]$
v_x	Vehicle longitudinal velocity	$[m/s]$
w_x	Longitudinal wind component	$[m/s]$
w_y	Crosswind component	$[m/s]$
w_y^{end}	Gust end amplitude	$[m/s]$
w_y^{max}	Gust maximum amplitude	$[m/s]$
w_y^{min}	Gust minimum amplitude	$[m/s]$
w_y^{start}	Gust end amplitude	$[m/s]$
δ_f	Front axle steer angle	$[rad]$
δ_r	Rear axle steer angle	$[rad]$
δ_{sw}	Steering wheel angle	$[rad]$
$\vec{\omega}$	Vehicle body angular velocity vector	$[deg/s]$
ω_x	Roll velocity	$[deg/s]$
ω_z	Yaw velocity	$[deg/s]$
ω_{xm}	Platform roll velocity	$[deg/s]$
ω_{zm}	Platform yaw velocity	$[deg/s]$
a_c	Centripetal acceleration	$[m/s^2]$
a_y	Lateral acceleration	$[m/s^2]$
a_{ym}	Platform lateral acceleration	$[m/s^2]$
dy	Lateral displacement	$[m/]$
h	Centre of gravity height	$[m]$
L	Wheel base	$[m]$

m	Vehicle mass	$[kg]$
t	Time	$[s]$
ρ	Density of air	$[kg/m^3]$
\dot{v}_y	Derivative of lateral velocity	$[m/s^2]$
ψ	Relative flow angle	$[deg]$
Δ	Change	

Contents

Nomenclature	viii
1 Introduction	1
1.1 Aim	3
1.2 Limitations and scope	3
1.3 Specification of issue under investigation	4
2 Background	5
2.1 Crosswind gusts	5
2.1.1 Crosswind gust parameters	6
2.1.2 Crosswind aerodynamic flow conditions and loads	7
2.2 Complexity and coupling	9
2.2.1 Mid-fidelity model	9
2.2.2 Coupling	10
2.3 Vehicle objective metrics	11
2.4 Driving simulator	12
2.4.1 Driver in loop Simulation	12
2.4.2 Virtual test track	12
2.4.3 Motion cueing	12
2.4.4 Audio, visual and haptic feedback	13
2.5 Driver safety and test duration	13
3 Methodology	14
3.1 Virtual vehicle model	14
3.2 Crosswind profiles	16

3.3	Simulink CRT interface	18
3.4	Single gust simulation	20
3.5	Vehicle and aerodynamics model validation	21
3.6	Realistic crosswind implementation	23
3.7	Subjective assessment	26
3.8	Subjective trigger	27
3.9	Objective metrics	28
3.10	Driving clinic and blind test	30
3.11	Hypothesis test	31
4	Results & Discussion	33
4.1	Subjective assessment	34
4.2	Subjective trigger statistics	35
4.3	Blind test statistics	36
4.4	Hypothesis test outcome	38
4.4.1	Null hypothesis test with all driver data	38
4.4.2	Null hypothesis test with driving data after blind test filter	39
4.5	Objective metrics rejecting hypothesis	41
4.6	Proxy signal amplitude to evaluate overall vehicle crosswind sensitivity	48
5	Conclusion	50
5.1	Future scope	51
	Bibliography	53
A	Appendix 1	I
A.1	Vehicle response to standard crosswind gust of profile 3	I
B	Appendix 2	III
B.1	Subjective assessment and questionnaire form	IV
C	Appendix 3	V
C.1	Driving clinic objective vehicle signals and subjective triggers	V
D	Appendix 4	XII

D.1	Vehicle OM signal response classified by driver subjective trigger	XII
D.1.1	OM and ST at 120 <i>kph</i> test	XIII
D.1.2	OM and ST at 160 <i>kph</i> test	XVI
D.1.3	OM and ST at 200 <i>kph</i> test	XIX

1

Introduction

Automotive companies mainly focus on developing safe and reliable vehicles with good handling performance that inspire confidence in real world driving environment. A vehicle with good aerodynamic stability has low sensitivity to crosswinds at all operating speeds, and it is crucial at high speeds for a driver to feel confident driving in straight highway lanes. Even in developing a high-level autonomous driving vehicle platform, the safe and stable motion of the vehicle will incline positively towards occupant safety, comfort, and efficiency.

Vehicle aerodynamics is an important response to environmental changes in high-speed driving scenarios. The aerodynamic characteristics are evaluated on test tracks and on roads, the change in geography and roadside structures around the highways creates wind disturbances which are known as crosswinds. High-speed aerodynamic stability tests are conducted later in development processes using development mules or prototypes. A change in the design requirement at the end of the development process will affect the limited design alternatives. The budget in terms of time and resource to allow late design changes is too expensive.

Current vehicle platforms are capable of being driven at high speeds in most highways, and thus aerodynamic behaviour and design are crucial. To improve these analysis it is essential to understand the aerodynamic behaviour of the vehicle to crosswinds that affect handling and driving comfort. Computer aided engineering (CAE) tools allow engineers to simulate real world crosswinds on cluster or on super computers dedicated to computational fluid dynamics (CFD) [1].

The passenger vehicle aerodynamics is primarily focused on reducing air drag coefficients, optimising lift forces and aerodynamic pressure balance between the axles. In real world, the wind direction cannot be predicted and these conditions change when travelling at high speeds. Crosswinds are present everywhere and therefore it is a priority to design vehicle aerodynamic properties around all types of wind conditions. Traditionally, the wind tunnel tests are done to find aerodynamic responses in constant flow conditions. Vehicle crosswind stability is tested with ISO standard tests, while these test crosswind parameters are limited to extreme conditions of crosswinds [2]. Accurate road wind conditions were studied and suggested a large deviation in the crosswind flow condition between the real world and ISO test flow conditions [1] [3].

Thus, offline simulation to study crosswind response of the vehicle is important for the overall development of the vehicle high speed characteristics. The offline simulations benefits the vehicle development immensely, but its time consuming and the subjective evaluation of the vehicle is not possible in offline simulation.

A driving simulator supports vehicle development at early stages as the CAE tools are to subjectively understand the vehicle's performance in a supervised virtual environment called driver-in-loop (DIL) simulation. It allows a driver to provide subjective assessment of the vehicle's behavior and its performance in test case scenarios before building a prototype vehicle. Driving simulators have excellent accuracy and repeatability, which enables engineers to run multiple scenarios and a large number of design configurations at the early stages of the development in a short duration at lower costs compared to the traditional prototyping approach at the end of the development process. The driving simulator works with sensory inputs namely haptic, visual and auditory feedback with good synchronisation and low latency between these feed backs sensory feedback delay between motion cueing benefit DIL simulation at the development [5].

A case study of DIL simulation of driving stability during crosswinds on Cruden 6 DOF driving simulator was conducted at Chalmers University of Technology. The driving clinic provided insight into the importance of latency between driver input and motion cueing in their subjective assessment. The visual quality of the virtual environment help the driver to feel immersed in the simulation. Additionally, the complexity of the model used for the simulation showed a large deviation in the objective measures in the DIL simulation [4].

At CEVT AB, the state-of-the-art VI-grade DIM250 driving simulator provides the best platform to bridge the knowledge gap required to test aerodynamics in the vehicle dynamics driving simulator for high-speed crosswind scenarios. This promotes the evaluation of the concept of safe and reliable aerodynamic vehicles in the early stages [6].

1.1 Aim

The primary focus of this thesis work is to implement crosswind gusts in high-speed driving scenarios in a driver-in-loop simulation. Secondly, investigate the correlation between vehicle response objective metrics and driver subjective feedback, also to define the region of instability and drivers subjective sensitivity in terms of vehicle objective measure.

1.2 Limitations and scope

- The project will not include any on-road testing, and testings are done on desktop simulation or on a driving simulator.
- The project uses cross-wind gust data observed at high-speed cross-wind testing done Hällered Proving Ground[7].
- The project will not perform any CFD simulations, the aerodynamic loads and models will be provided to the students by the company.
- A prototype Lynk&Co 01 vehicle dynamics model is used for the desktop CAE simulation and the same vehicle dynamics model is used in the driving simulator for the DIL simulation.
- Common and experienced drivers in the driving clinic are CEVT employees.
- The driver feedback from the DIL simulation is based solely on the driver experience.
- The motion cueing algorithm used for the study is tuned for a good subjective lateral dynamic feel by the company.
- The steering feedback torque and the model used in the vehicle model is provided by the company.
- The statistical analysis and its results are completely based on the recorded data.

1.3 Specification of issue under investigation

The objective of this thesis work is to understand the usefulness of the driver in loop simulation. The initial task was to implement the vehicle model in the driving simulator with dynamic and aerodynamic coupling of the vehicle. Secondly, to find the correlation between subjective assessment and vehicle objective measures.

The following research questions were constructed to guide this study:

- What level of complexity is needed for the coupled vehicle dynamic and aerodynamic models to evaluate crosswind sensitivity in the driving simulator?
- How realistic is the vehicle response to high-speed crosswind gust implementation?
- How does the subjective assessment of the vehicle changes with increasing test speed?
- What objective vehicle response to crosswind gust disturbance correlates with driver subjective feedback?
- What vehicle response amplitudes can drivers detect, and at what levels do they classify as stability issues?

2

Background

This chapter provides insight into the crosswind gusts and its profiles in Section 2.1.1. The aerodynamic model for accurate flow conditions & loads on the vehicle during high-speeds are discussed in 2.1.2. The vehicle model complexity and coupling method used in the simulations are shown in 2.2. To understand the change in vehicle response, the objective metrics of the vehicle 2.3 are briefly discussed. The driving simulator tools and the driving feedback system used in the study are discussed along with the psychophysiology of the driver and the duration of the test, which are briefly discussed in 2.4 and 2.5.

2.1 Crosswind gusts

Crosswind gusts are change in wind amplitudes that flow perpendicular to the direction of travel. The unstable wind flow condition occurs due to turbulent flow in the natural wind and disturbances caused by other road vehicles, which also involve obstacles on the roadside. From the above three mentioned components affecting wind flow, the roadside obstacles have the largest consequences that causes highly unsteady crosswind gusts. At high speeds, the vehicle often crosses obstacles on the road, and small to large crosswind disturbances occur. In Wojciak [3] study, the crosswind gusts are classified into three types such as large turbulence scales with quasi-steady effect, medium turbulence scales with relevant effect and small turbulence scale with irrelevant scale. In the Wojciak study [3], it is observed that the wind flow angles between 5 and 9 degrees at a vehicle speed of 140 km/h are more sensitive and cause driving instability. The crosswind gust flow conditions directly affect the aerodynamic loads on the vehicle, and vehicle dynamics is effected indirectly at the same magnitude.

2.1.1 Crosswind gust parameters

The wind data from the Hällared proving ground provides an idea of the magnitude and direction of flow of the wind gusts while driving at high speeds. Crosswinds have different magnitudes, and their intensity is explained as a Beaufort wind scale [10]. The crosswind gusts are never similar as a result of the unstable nature of the natural wind. When visually examined, the crosswind gusts are classified on the basis of the patterns, which are called profiles in the study. These patterns are mathematically defined as the function shown in 2.1. In this function, the crosswind gust profile is based on the amplitude and time duration of the gust. The amplitude of the gust is controlled by four parameters ie w_y^{start} , w_y^{end} , w_y^{max} , w_y^{min} and the duration of the gust of the crosswind is based on four parameters t_0 , t_b , t_p , t_d . The wind parameters are shown below in the table 2.1

Parameters	Symbols
Time	t
Gust start time	t_0
Gust build up time	t_b
Gust pause time	t_p
Gust drop time	t_d
Crosswind component	w_y
Gust start amplitude	w_y^{start}
Gust end amplitude	w_y^{end}
Gust maximum amplitude	w_y^{max}
Gust minimum amplitude	w_y^{min}

Table 2.1: Crosswind parameters

$$w_y(t) \left\{ \begin{array}{l}
= w_y^{\text{start}} \\
\text{for } t < t_0 \\
\\
= w_y^{\text{start}} + \frac{w_y^{\text{max}} - w_y^{\text{start}}}{2} \left(1 - \cos \left(\frac{\pi}{t_b} (t - t_0) \right) \right) \\
\text{for } t_0 < t < t_0 + t_b \\
\\
= w_y^{\text{max}} \\
\text{for } t_0 + t_b < t < t_0 + t_b + t_p \\
\\
= w_y^{\text{max}} - \frac{w_y^{\text{max}} - w_y^{\text{min}}}{2} \left(1 - \cos \left(\frac{\pi}{t_d} (t - t_0 - t_b - t_p) \right) \right) \\
\text{for } t_0 + t_b + t_p < t < t_0 + t_b + t_p + t_d \\
\\
= w_y^{\text{min}} \\
\text{for } t_0 + t_b + t_p + t_d < t < t_0 + t_b + 2t_p + t_d \\
\\
= w_y^{\text{end}} + \frac{w_y^{\text{min}} - w_y^{\text{end}}}{2} \left(1 + \cos \left(\frac{\pi}{t_b} (t - t_0 - t_b - 2t_p - t_d) \right) \right) \\
\text{for } t_0 + t_b + 2t_p + t_d < t < t_0 + 2t_b + 2t_p + t_d \\
\\
= w_y^{\text{end}} \\
\text{for } t > t_0 + 2t_b + 2t_p + t_d
\end{array} \right.$$

Figure 2.1: Mathematical gust function
[8]

2.1.2 Crosswind aerodynamic flow conditions and loads

The crosswind gusts are applied on the vehicle based on the flow angle of the crosswind, the relative vehicle and wind velocities, this is called the relative flow condition. The aerodynamic coefficients of the vehicle vary when the relative wind flow angle changes, and the aerodynamic coefficients obtained from unsteady CFD simulation at various wind yaw angles, provided by CEVT, change with flow conditions. The flow condition of the wind and the aerodynamic coefficients with parameters such as L wheelbase, A_f frontal cross-sectional area of the vehicle and ρ the density of the air with relative magnitude of velocity of the vehicle V_{mag} used to model the aerodynamic forces and moments are as shown in the below equations 2.1,2.2,2.3,2.4,2.5 2.6.

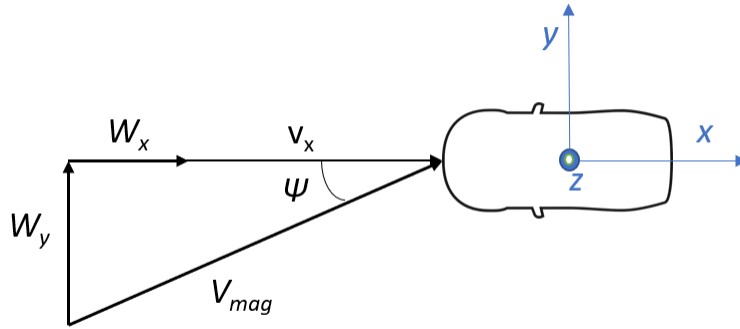


Figure 2.2: Crosswind flow angle and velocity components with vehicle velocity component forming flow condition of the crosswind

$$F_d = \frac{1}{2} * \rho * A_f (C_d * V_{mag}^2) \quad (2.1)$$

$$F_s = \frac{1}{2} * \rho * A_f (C_s * V_{mag}^2) \quad (2.2)$$

$$F_l = \frac{1}{2} * \rho * A_f (C_l * V_{mag}^2) \quad (2.3)$$

$$M_x = \frac{1}{2} * \rho * A_f * L (C_{rm} * V_{mag}^2) \quad (2.4)$$

$$M_y = \frac{1}{4} * \rho * A_f * L (C_{pm} * V_{mag}^2) \quad (2.5)$$

$$M_z = \frac{1}{4} * \rho * A_f * L (C_{ym} * V_{mag}^2) \quad (2.6)$$

Forces and moments are implemented on the vehicle considering the axle delay, and loads are applied at the point exactly between the axles at the center of the wheel base line, the same reference point as the coefficients obtained from the unsteady CFD simulation at various wind angles. The directions of the forces and moments are in the aerodynamic reference system and later changed into the vehicle dynamics coordinate system, as shown in figure 3.3.

2.2 Complexity and coupling

The complexity and coupling are most important part in developing the vehicle model and evaluating the fitness of the CAE or DIL simulation with the real world scenarios.

2.2.1 Mid-fidelity model

The vehicles dynamic models are responsible for reproducing the response of the real vehicle in a virtual environment with good accuracy. The dynamics of the vehicle chassis, suspension and steering all together increases the complexity in vehicle dynamics, further complicated with powertrain models. Thus, the use of high complexity model requires high computational time and accurate vehicle design parameter to give real world correlating vehicle response. Low-fidelity models are not detailed enough for good accuracy for this study because the low degree of freedom in the vehicle model dampens vehicle responses compared to medium or high complexity models. The mid-fidelity is balanced with enough complexities to emulate the real vehicle response with good accuracy, and further complexities can be added to improve the vehicle model. The mid fidelity model is used to compare the vehicle response from the CAE tool and is explained in the next chapter 3.5.

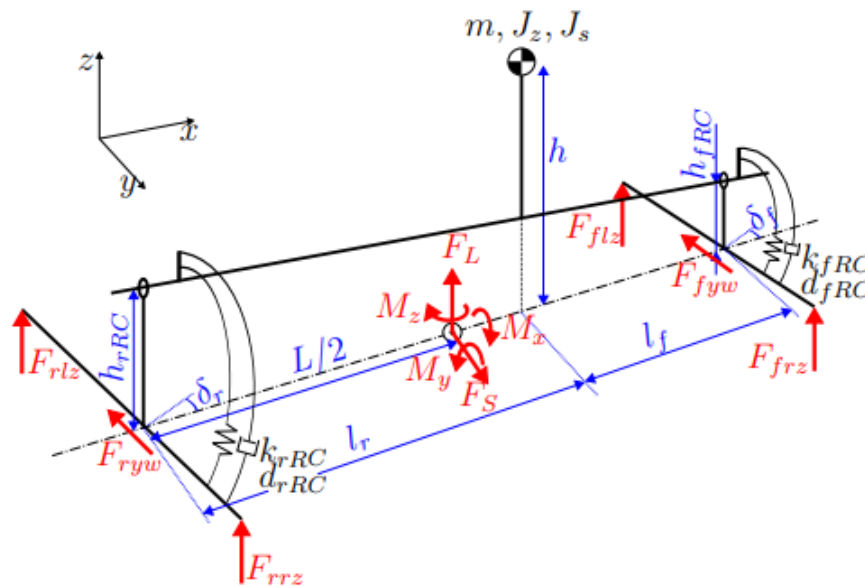


Figure 2.3: Mid-fidelity model

2.2.2 Coupling

The coupling between aerodynamics and vehicle dynamics is implemented in three methods, as shown in Figs. 2.4, 2.5, and 2.6. In one-way coupling, the response to vehicle motion is influenced by the aerodynamics and vehicle dynamics of the vehicle model, but the aerodynamics model does not consider changing the dynamic motion of the vehicle caused by itself. In two-way coupling, the aerodynamic model flow conditions are based on vehicle dynamic responses using vehicle longitudinal and lateral velocities as body slip. Here, the crosswinds are perpendicular to the vehicle.

In an improved two-way coupling, the flow condition uses the relative change in the yaw angle of the vehicle with respect to the road in the x-axis or longitudinal direction. Body slip and yaw angle control flow conditions when there is a large change in yaw response of the vehicle due to crosswind gust or the driver steering excitation. This can be visualized as the crosswind gusts defined perpendicular to the road and not to the vehicle.

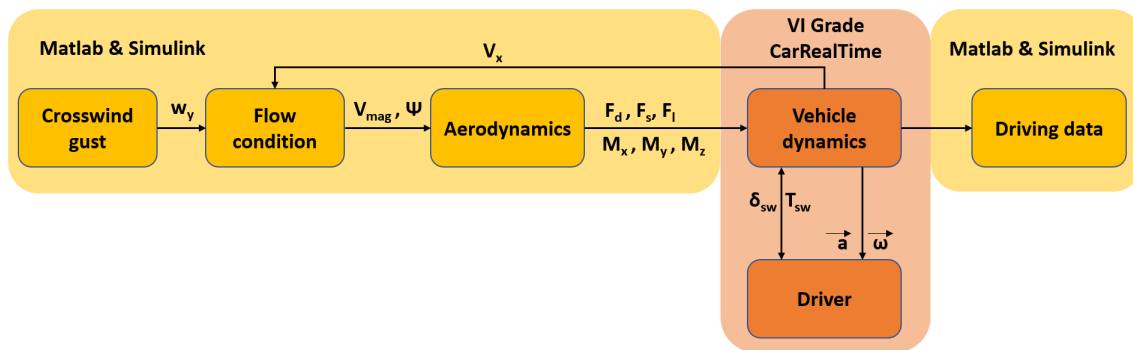


Figure 2.4: One way coupling to simulate flow conditions of crosswinds defined on the vehicle reference point without considering vehicle dynamic responses

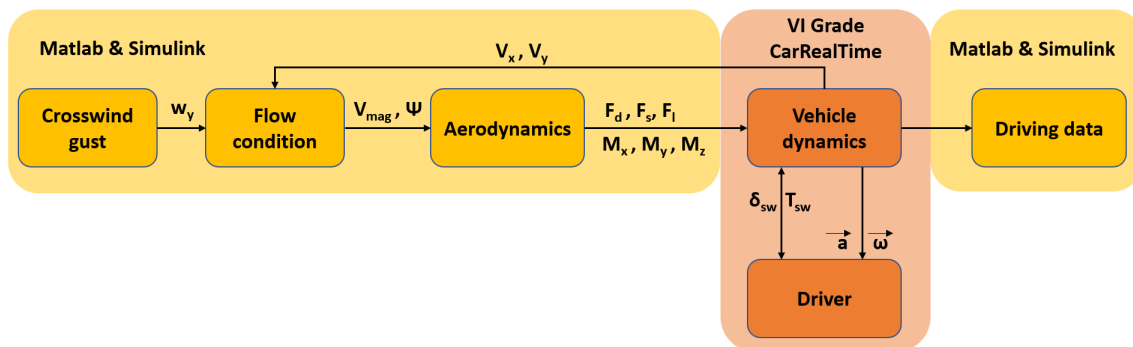


Figure 2.5: Two way coupling to simulate flow conditions of crosswinds defined perpendicular to the vehicle in the road plane

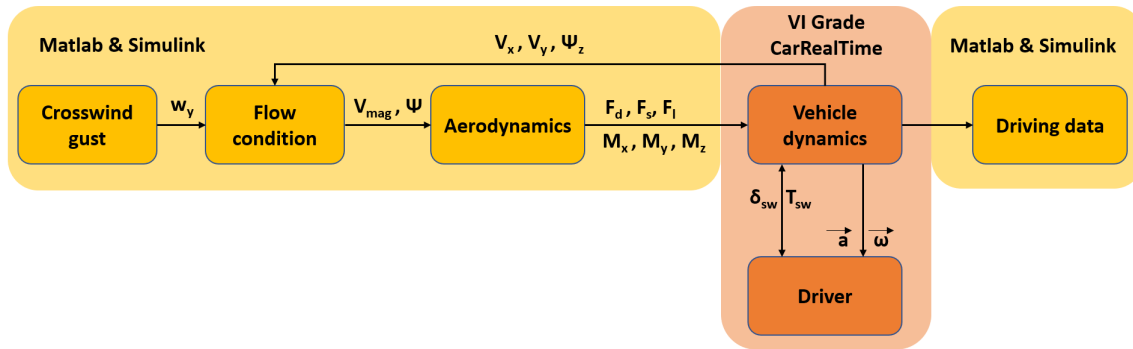


Figure 2.6: Improved two-way coupling to simulate the flow conditions of the crosswinds perpendicular to the road for large yaw angle change

2.3 Vehicle objective metrics

The vehicle performance is evaluated by understanding change in vehicle response for a change in vehicle design parameters or test parameters. The objective metrics provide insight into the change in performance and give direction to the development process of a prototype vehicle or to improve a vehicle model to a certain benchmark. ISO standards [2] recommend objective metrics for the study of crosswind sensitivity. Their standardized test analyzes the vehicle yaw angle, lateral acceleration and yaw velocity response, the path deviation is also measured using dye-trail method or other computational method. The crosswind sensitivity study often deviates because the wind tunnel test flow parameters are different from the real-world wind conditions. Meanwhile, the ISO tests are conducted in real world where the wind conditions keep varying through time and distance, thus proving difficult to engineers to understand the vehicle aerodynamic and vehicle dynamic response in crosswind study. Although this study is primarily focused on high-speed straight line driving under crosswind gusts and in a virtual environment, vehicle signals are recorded to study the vehicle performance and understand driver perception of stability. Few of the most important benefits of CAE simulations are accuracy and repeatability which directly improves reliability of objective metrics. In a study by Huemer.J on the influence of unsteady aerodynamics [14] it is clearly shown that vehicle responses such as lateral acceleration, yaw velocity and roll velocity are sensitive to crosswind disturbances. Also, in a study related aerodynamic excitation [15] shows that the drivers are sensitive to yaw disturbances more than the roll disturbances during crosswind gusts.

2.4 Driving simulator

The thesis work is carried out on the CEVT AB's VI-grade DIM250 driving simulator. Currently, driving simulators provide great support in developing and improving vehicle design and evaluating performance at an early stage. The benefit of using a driving simulator in the development process is the feedback from a driver through subjective assessment of the vehicle design iteration while it provides a safe testing environment, where extreme and different conditions can be tested virtually and provide vehicle response with great accuracy and repeatability. Additionally, a driving simulator allows the study of driver behavior and driving input that affect vehicle response.

2.4.1 Driver in loop Simulation

Driver in loop (DIL) simulations, also known as online simulations involves a real driver in the simulation process. While desktop or off-line simulations use a virtual driver model, a driving simulator uses a real driver and considers their input in the virtual simulation. The DIL simulation is used to measure vehicle performance and understand subjective feeling to examine and understand the vehicle development process in the very early stages of the development process [4].

2.4.2 Virtual test track

A virtual test track from VI grade is used for the crosswind gust event simulation. The test track is an infinitely straight highway road and this helps the study to run the driving simulation for any required amount of time. These test tracks include environmental graphics such as trees, hills, bridges and road signs. This makes the driver more involved and provide realistic driving experience. The road profile noises are controllable, which is in sync with the cockpit shakers.

2.4.3 Motion cueing

Motion cueing moves the driving cockpit to replicate real driving disturbances on the driver to evaluate the vehicle model on the driving simulator. Motion cueing algorithm controls the actuators, and the vibrators (shakers) on a moving base platform creates road and engine noise vibration into the cockpit. The limited 6 degrees of freedom hexapod moves with the platform to create forces and moments on drivers. Motion cueing plays an important role, working in conjunction with other cues such as haptic, visual, and audio feedbacks to immerse the driver and achieve a realistic driving

experience. The limitation of the space and force of actuators of the motion platform makes it difficult to obtain the exact motion of the vehicle model on the driving simulator. Therefore, the motion cueing algorithm allows giving near-realistic feedback and is indeed a best way to simulate disturbances to the driver [11] and [5].

2.4.4 Audio, visual and haptic feedback

Audio feedback is provided by the speakers in the driving cockpit. Since the driving simulator has a closed cockpit, external noises from the moving platform and the actuators are completely unnoticeable. The visual feedback provides sensory input to the driver on a conical screen and it plays a major role in immersing the driver to reduce motion sickness. The simulator has a fixed 8-9m conical screen with best visual immersion quality that results in better visual input to the driver. Conical screens provide the effect of stereoscopic vision that improves the quality of visual feedback. The immersive display graphics projected on the screen and the cockpit motion with low latency improves the quality of DIL simulation. Motion cues with audio and visual feedback provide complete sensory input to the driver, while haptic feedback allow driver to understand the vehicle response through steering feedback. Based on the cockpit steering angle, the steering wheel feedback torque is generated and road noise vibrations are fed through the steering wheel torque and cockpit simulator. The VI-grade DIM 250 simulator provides the best DIL simulation with the lowest latency between all the above-mentioned feedback.

2.5 Driver safety and test duration

In a DIL simulation, the subjective assessment of the driver should be accurate and reliable for testing the handling and behavior of a vehicle. Motion cueing affects differently for each driver based on his or her experience in the driving simulator and the psychophysiology of the driver. A driver sensitive to motion sickness is affected by deterioration of mental alertness due to fatigue and awareness [16]. The driving experience is improved by inducing road noise in the cockpit [18] and the audio, visual, steering feedback with good motion cueing setup with low latency interaction.

The psychological and physiological behavior of the driver when undisturbed while driving; The driver cannot accurately perform the subjective evaluation due to monotonous straight-line driving [17]. A similar study for straight-line high-speed driving [15] suggests less than 20 minutes for a driving session. The driving clinic considers all drivers' safety to obtain reliable subjective assessment.

3

Methodology

This chapter overviews the implementation of crosswind gusts into the driver in loop simulation. Firstly, the virtual vehicle model used in the study is discussed in section 3.1 and also insight into the different crosswinds profiles are provided in the Section 3.2. The platform where crosswind gusts are implemented into CarRealTime is presented in the Section 3.3. To evaluate vehicle complexity, vehicle responses for single crosswind gusts and vehicle model validation of CRT and mid-fidelity vehicles are discussed in Sections 3.4 and 3.5, respectively.

The DIL simulations are improved by the development of randomised crosswind gusts implementation is described in the Section 3.6. The necessary objective metrics and subjective assessment tools with procedure to conduct successful driving clinic are elaborated in Sections 3.7 to 3.10. The statistical method used to correlate and study the subjective feedback of the driver is presented in Section 3.11.

3.1 Virtual vehicle model

The virtual vehicle model or the CRT vehicle model shows the vehicle response of the prototype SUV, the vehicle dynamic and aerodynamic parameters are provided by CEVT AB for the study.

First, a mid-fidelity model (mathematical model) is set with real-world parameters, and vehicle responses are compared [1]. The response to crosswind gusts of the vehicle is entirely based on the vehicle parameters. The parameters of mid-fidelity model are discussed in the table 3.5 below and tested for close fitness with the CRT vehicle model.

The CRT vehicle model is a complex model consisting of various vehicle dynamics models such as propulsion system models, tyre models, chassis model, steering model and suspension model. From the aerodynamics unsteady CFD data provided by CEVT AB and the aerodynamics model is coupled to vehicle dynamics model as discussed in Section 2.2.2.



Figure 3.1: Vehicle used in the study

Parameter	Data
Vehicle	Lynk&Co 01 (SUV)
Transmission	Front wheel driven (Automatic)
Length	4.51m
Height	1.86m
Wheel base	2.73m
Kerb weight	1856kg
Tire	235/50 R19
Front suspension	MacPherson
Rear suspension	4-link trailing arm

Table 3.1: Vehicle parameters

3.2 Crosswind profiles

In the nature, crosswind gusts are turbulent and have unsteadiness behavior. The variation in these crosswinds can be broken down into varying amplitude and time duration. As mentioned in the previous Section 2.1.1, from the patterns or profiles of crosswind gusts observed at the Hällared proving ground, the gusts obtained are grouped into three types of profiles.

- **Profile 1:** The crosswind gust amplitude is initially at zero w_y^{start} , the amplitude is built to the maximum w_y^{max} crosswind in the build time t_b and then at the same duration, it changes the direction of the amplitude toward the minimum w_y^{min} . This profile then drops to zero w_y^{end} at a drop duration t_d .
- **Profile 2:** This profile is similar to profile1 and is identified as slow build-up and rapid drop crosswind. But one major difference in this type of profile is that the build-up time is much less than in profile 1. This rapid drop in the time causes significant issues in the vehicle.
- **Profile 3:** In contrast to the two profiles above, this profile has a considerably longer pause duration without any zero crossing. The quick ramp up and ramp down in time duration with higher amplitudes makes it unrealistic with the natural crosswind conditions.

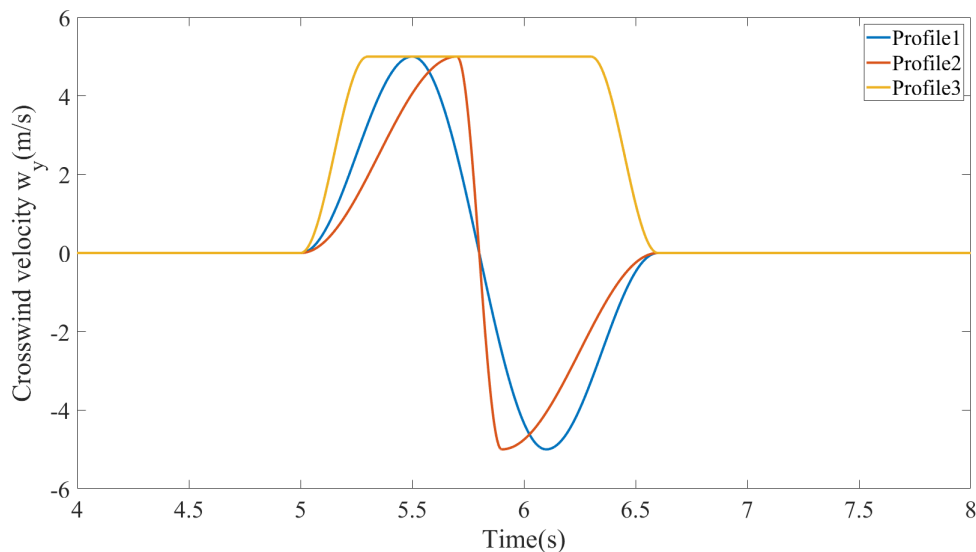


Figure 3.2: Crosswind gust profiles

	Profile 1	Profile 2	Profile 3
$w_y^{\text{start}}[\text{m/s}]$	0	0	0
$w_y^{\text{max}}[\text{m/s}]$	5	5	5
$w_y^{\text{min}}[\text{m/s}]$	-5	-5	5
$w_y^{\text{end}}[\text{m/s}]$	0	0	0
$t_b[\text{S}]$	0.5	0.7	0.3
$t_p[\text{S}]$	0	0	0.5
$t_d[\text{s}]$	0.6	0.2	0
$t_{\text{gust}} = 2t_b + 2t_p + t_d[\text{S}]$	1.6	1.6	1.6

Table 3.2: Standard crosswind gusts profile parameters

3.3 Simulink CRT interface

The crosswind gust velocities are mathematically generated on simulink with the gust parameters. The flow condition is dictated by the relative velocity between the crosswind and the vehicle. Flow condition and the yaw angle relative aerodynamic coefficients of the vehicle model from unsteady CFD simulation gives aerodynamic loads [7]. The aerodynamic loads changes with crosswind gust velocity, vehicle velocity and yaw angle on simulink interface, these input aerodynamic load signals as shown in table 3.4 are fed into vehicle dynamics block of the CRT vehicle model on simulink following the relation shown in table 3.3. The varying aerodynamic loads on straight-line driving gives a transient vehicle dynamic response on CRT simulation with a standard driver model to follow a straight lane. The vehicle- aerodynamic coupling signals shown in table 3.4 are feedback from CRT vehicle dynamics to the flow condition block on simulink.

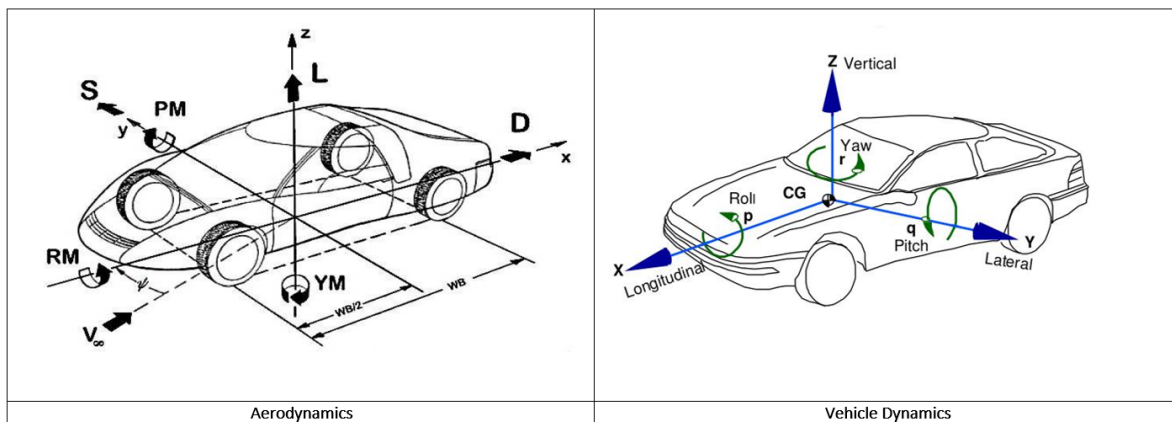


Figure 3.3: Aerodynamics and vehicle dynamics coordinate system [13]

Forces and moments	Aerodynamics	Vehicle dynamics	Relation
Drag force	F_d	F_x	$F_d = -F_x$
Side force	F_s	F_y	$F_s = -F_y$
Lift force	F_l	F_z	$F_l = F_z$
Roll moment	M_x	M_x	M_x
Pitch moment	M_y	M_y	$-M_y$
Yaw moment	M_z	M_z	$-M_z$

Table 3.3: Sign convention for aerodynamics and vehicle dynamics system

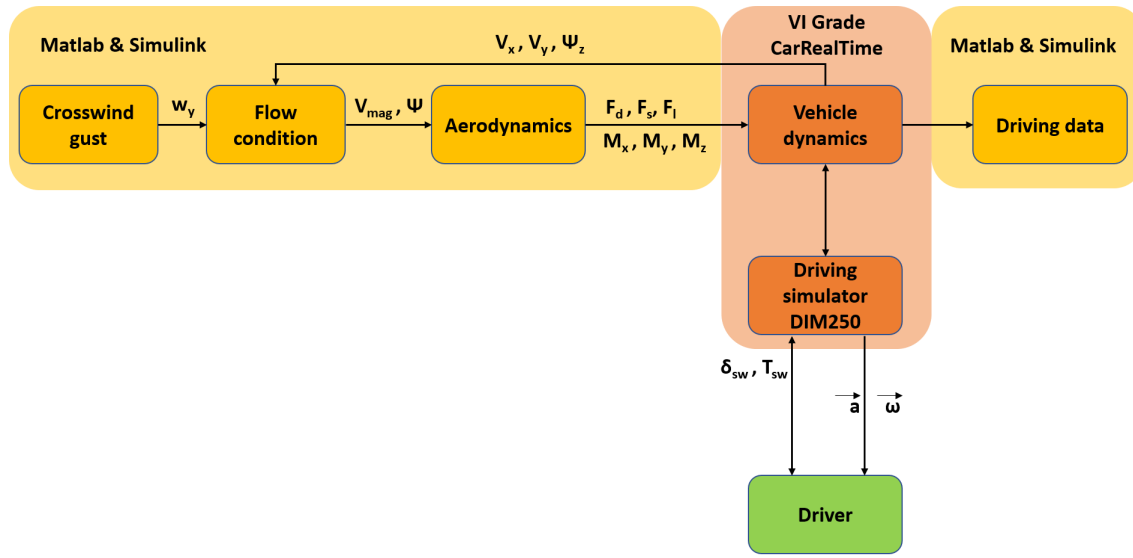


Figure 3.4: Simulink and CRT Interfaces

The vehicle dynamic block is setup by parameters of vehicle models, maneuver definition, driver model and environment or road scenario .

Sl.no	Input signals	Output signals
1	Aerodynamic drag force at center	Lateral velocity
2	Aerodynamic side force at center	Longitudinal velocity
3	Aerodynamic lift force at center	Yaw angle
4	Aerodynamic roll moment	
5	Aerodynamic pitch moment	
6	Aerodynamic yaw moment	

Table 3.4: CRT and Simulink interface signals for aerodynamic flow conditions

3.4 Single gust simulation

The aerodynamic loads for single crosswind gusts are calculated for the flow conditions that are induced perpendicular to the straight road. The wind flow condition signals i.e. v_{mag} and ψ are split into front and rear axle. The unsteady CFD data for coefficients of forces and moments are relative to the ψ angle (wind yaw angle). The coefficients of drag, side, lift forces, and roll, pitch & yaw moments are calculated and fed into the vehicle dynamic model. Thus, aerodynamic loads that vary according to changing wind flow conditions with axle delay improves the driving experience and vehicle response to the crosswind gust.

The following graphs are the responses of the CRT simulation vehicle of a single event of crosswind gusts for different profiles while driving at a speed of $160kph$ at zero steering angle. The vehicle lateral acceleration, yaw & roll velocities, steering wheel torque are shown in the figures 3.5, 3.6, 3.7, 3.8.

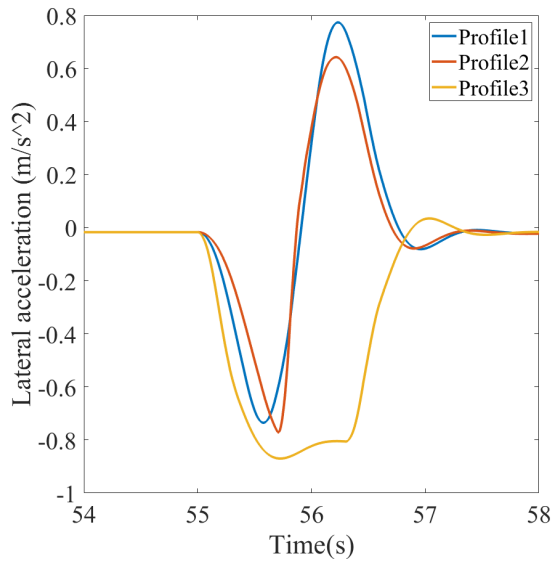


Figure 3.5: Vehicle lateral acceleration response during single crosswind event for different profiles

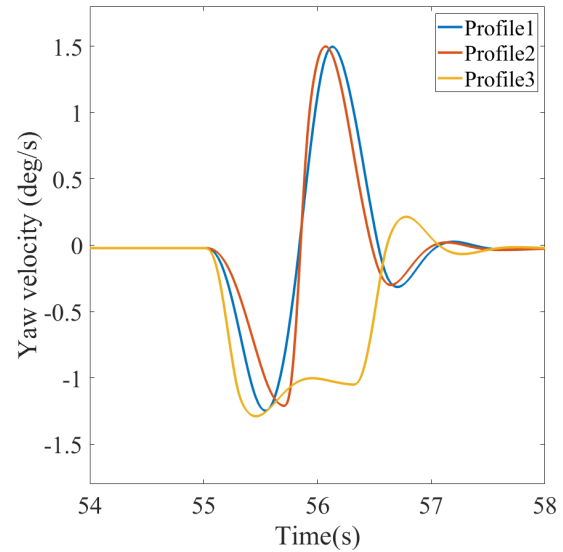


Figure 3.6: Vehicle yaw velocity response during single crosswind event for different profiles

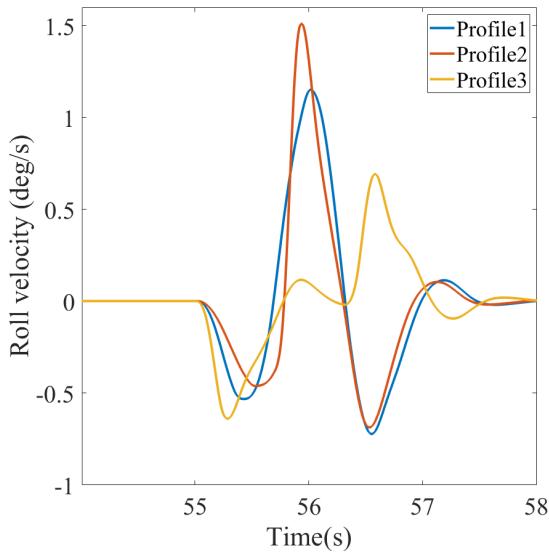


Figure 3.7: Vehicle roll velocity response during single crosswind event for different profiles

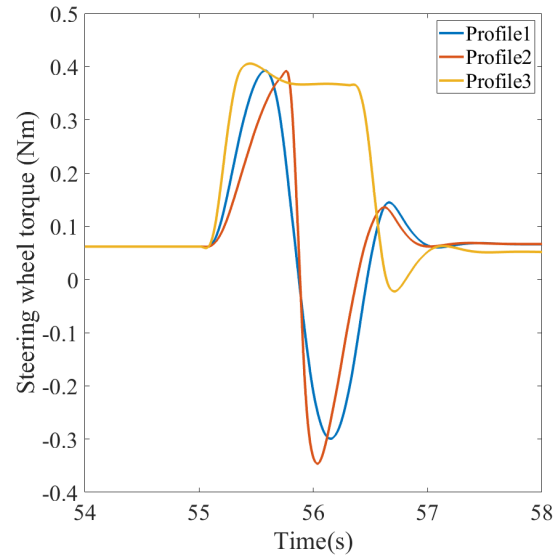


Figure 3.8: Vehicle steering wheel torque response during single crosswind event for different profiles

3.5 Vehicle and aerodynamics model validation

The study [7] involved testing the real-world vehicle at high speeds testing crosswind gust response. Vehicle response and wind gust data obtained as explained in his research was transferred to virtual simulation to study vehicle aerodynamic instability. In addition, the real-world vehicle response was compared with low-fidelity, mid-fidelity, and high-fidelity models, which are in the order of complexities and degrees of freedom of the vehicle model. A comparison was established between these models and the mid fidelity model response had close fit with the real-world vehicle response. Thus, a mid-fidelity model has a good vehicle dynamic physics to replicate a real-world vehicle.

The vehicle model used in CRT simulation is obtained from CEVT AB and which is updated to have good fitness with the real-world vehicle. The CRT vehicle parameters when used in mid-fidelity model, the response of the mid-fidelity model for the crosswind gust should provide the same response from the CRT vehicle model for the same crosswind gust. This is to check the fitness of the CRT vehicle dynamic response for the same aerodynamic loads that the mid-fidelity model provides and this is because the mid-fidelity model has a well-established aerodynamic implementation in the vehicle dynamic model [7].

The vehicle responses such as lateral acceleration, yaw velocity and tire normal loads are

the most important vehicle signals to compare the vehicle dynamics and the crosswind gusts effect on vehicle dynamics. The parameters were initialized into a mid-fidelity model by testing the CRT vehicle in virtual simulation for mass, center of gravity position, and center of roll height in addition to the vehicle data provided from CEVT AB.

The CRT vehicle model and the mid-fidelity model response to a single crosswind gust of profile 1 are shown below in figures 3.9, 3.10 and 3.11 are compared. The CRT vehicle shows a close vehicle dynamic response to the mid-fidelity model, and thus it establishes correlation with the real-world vehicle. To get good fitness in response, the vehicle model parameters must be equal and accurate to real world vehicle. The 2-way coupling method implemented the crosswind gusts accurately on CRT simulation.

The vehicle responses between the CRT and the mid-fidelity vehicle model for crosswind gust profile 3 are compared and are shown in Appendix 1 A.

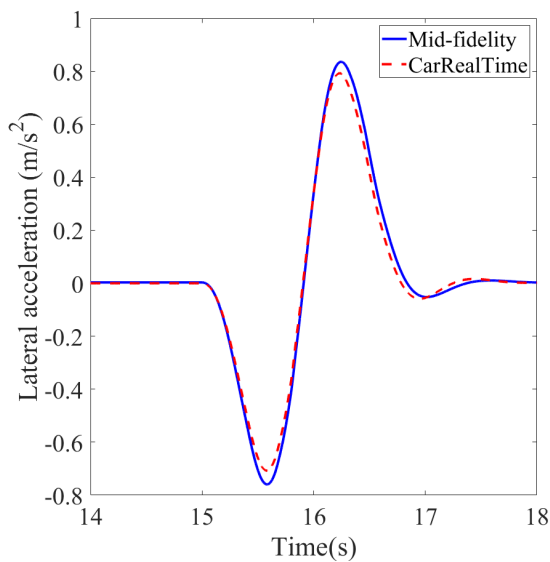


Figure 3.9: Lateral acceleration comparison between mid fidelity and CRT model

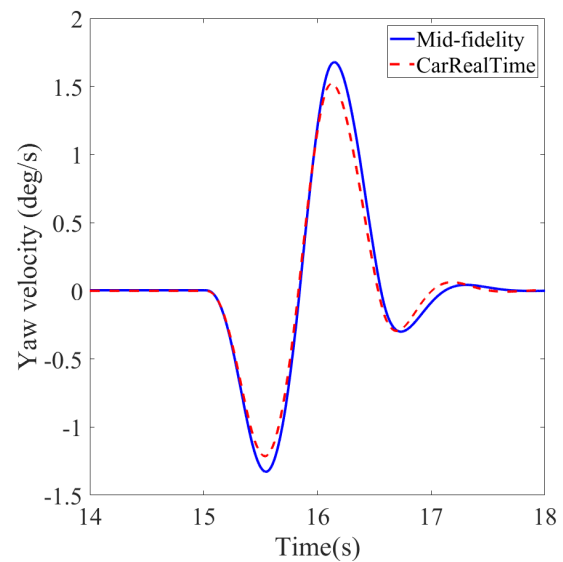


Figure 3.10: Yaw velocity comparison between mid fidelity and CRT model

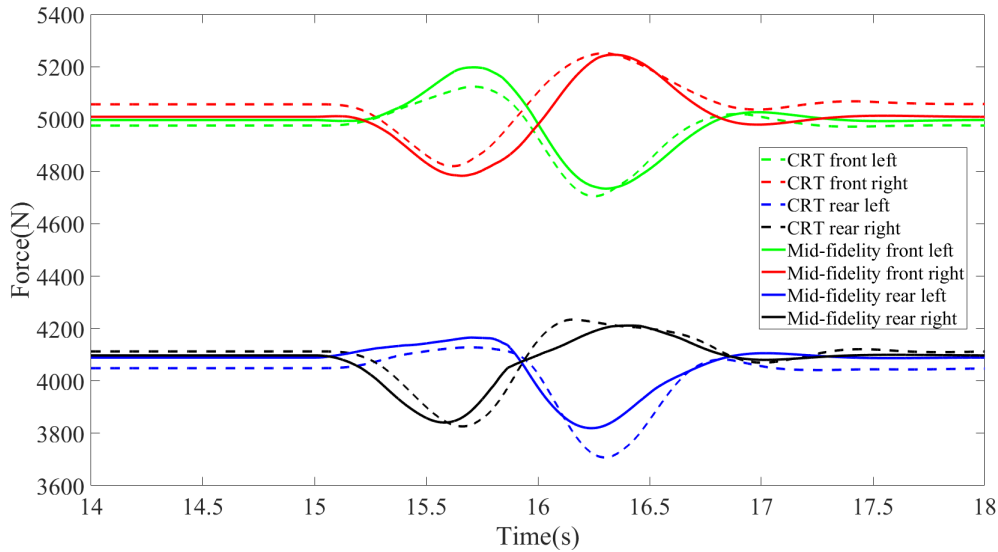


Figure 3.11: Tire normal loads comparison between mid fidelity and CRT model

3.6 Realistic crosswind implementation

The target of the DIL simulation is to obtain good driving data by implementing realistic crosswind disturbances for accurate subjective feedback. Initially, the implementation of the crosswind gust evaluates three different profiles, as shown in Figure 3.2 of the standard time duration, as explained in Section 2.1.1. These crosswind gusts were tested to find noticeable differences in the DIL simulation. The drivers subjectively reported that there was no noticeable difference in between the responses of the vehicle with gust profile 1 and 2. The crosswind profile type 1 and 3, i.e. crosswind with and without zero crossing parameters have very different vehicle responses and subjective feeling in the DIL simulation. In a similar study of crosswind gust implementation [4] the drivers felt the cockpit was floating in high speed straight line driving in crosswind DIL simulation.

Meanwhile, the drivers recognized the periodic nature and type of gusts after a single DIL simulation test. Randomization of the crosswind gust parameters allowed for close proximity to real-world crosswind gusts, which represents the stochastic nature. Thus, randomisation immensely benefited the crosswind gust scenario to immerse the driver in DIL simulation.

In the real world, straight-line driving at high speed is effected by crosswinds of small amplitudes at high frequency i.e. aerodynamic disturbances. The disturbances implemented in the crosswind gusts are stochastic and mathematically added to the crosswind

gust signals. The aerodynamic disturbance amplitudes and frequencies are tuned by the driver's intuition and feedback and are modeled similarly to crosswind gusts with axle delay. The axle delay is a function of vehicle velocity and wheelbase, and this evidently improved driver feedback.

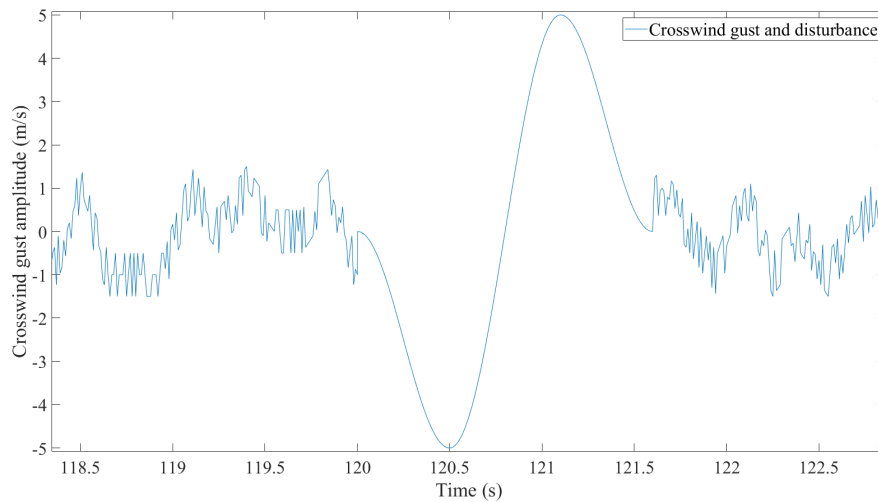


Figure 3.12: A single crosswind gust and small disturbances spliced over time

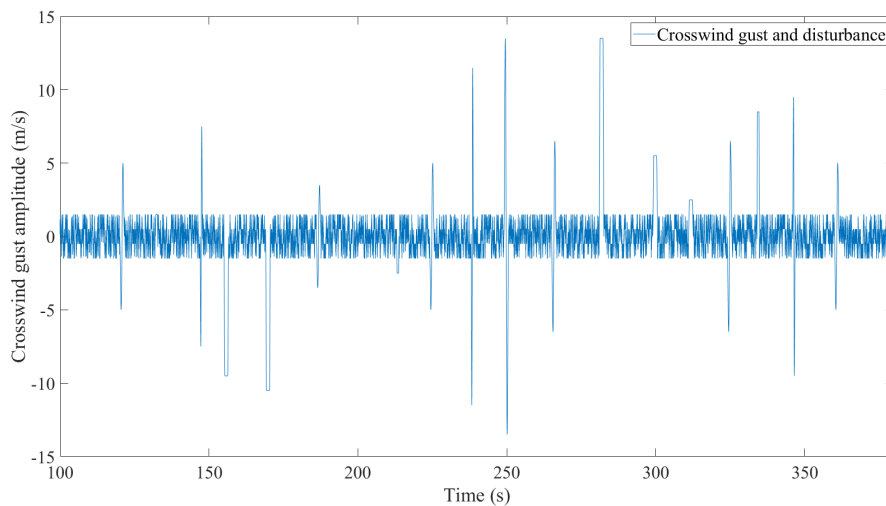


Figure 3.13: Crosswind gust event with randomised parameters with crosswind disturbances

A study on driver subjective perception during ride disturbance [18] shows that road noise plays important role in providing driver a good driving feedback and in this study

the wind noise are added on aerodynamic reference point with the aerodynamic loads on the vehicle during crosswind gust. Meanwhile, road, engine, chassis, and environment noise is controllable and can be adjusted to realistic road driving noise feedback. The DIM 250 cockpit is equipped with shakers that provide vibrations similar to real road driving noise.

The vehicle and driver response signals of DIL simulation for crosswind gust event with randomised series wind parameter and disturbances are shown in the Appendix C.

3.7 Subjective assessment

The subjective rating scale shown in the figure below 3.14 is used to correlate the SA of the driver and the performance of the vehicle by varying the wind gust parameters. The crosswind gusts affect the vehicle in lateral direction, vehicle behaviour addressing lateral crosswind stability and vehicle control responses are studied in 4.1.

		Event Type		
		Disturbance	Control	
Rating Scale	Desirable	10	Imperceptible	Excellent
		9	Trace	
		8	A Little	Good
		7	Some	
		6	Moderate	Fair
	5	Borderline		
	Undesirable	4	Annoying	Poor
		3	Strong	
		2	Severe	Very Poor
		1	Not Acceptable	

Figure 3.14: Subjective Rating Scale
[12]

DIL simulation allows engineers to understand vehicle handling behavior and characteristics using SA questionnaires. The questionnaires are focused to develop understanding of the vehicle responses in lateral control that a driver can perceive and are listed below.

- How is the vehicle straight path tracking?
- How is the vehicle yaw stability to the crosswind gusts?
- How is the vehicle roll stability to the crosswind gusts?
- How is the vehicle controllability during the crosswind gusts?
- How realistic is the crosswind gust event implementation?

3.8 Subjective trigger

To quantify the subjective feedback of the driver to disturbances of the wind gusts in terms of the vehicle response measure, the study develops a method to use numbers 0, 1, 2 and 3, each number subjectively defines the vehicle response to a gust to the driver. These numbers are called subjective triggers (ST) and are reported verbally from the cockpit mic for every crosswind gust implemented in DIL simulation tests. Drivers report the ST number based on the amplitude of vehicle response they subjectively feel. The subjective feeling of the disturbance due to the wind in a high-speed vehicle driving in a straight lane is predefined by the ST numbers shown below.

- **ST0**- The driver did not feel the crosswind gust. (Obtained while post processing the driving data)
- **ST1**- The driver felt the crosswind gust, but it did not affect the vehicle straight path following.
- **ST2**-The driver felt the crosswind gust mildly, the vehicle straight path following is affected but the vehicle is controllable.
- **ST3**-The driver felt the crosswind gust severely, the vehicle did not follow the intended path and is difficult to controllable.

The ST method allows a detailed study of regions of driver sensitivity to crosswind gust disturbance in terms of vehicle objective metric response. The ST statistics from the study is explained in Section 4.2 . The vehicle crosswind gust response signals are grouped based on the test speed and ST reported by the driver for testing the hypothesis as explained in Section 3.11.

3.9 Objective metrics

The OMs are vehicle response amplitudes that are tested to find correlation with the driver subjective assessment and trigger. The OM investigates the change in vehicle signals and driver input response; the peak-to-peak-amplitude vehicle response to crosswinds at different gust amplitudes are different. The magnitude of the change in vehicle response for a crosswind depends on the magnitude of change in aerodynamic loads on the vehicle. Therefore, to measure the effect of crosswind gust during high-speed driving at 120, 160 and 200 kph on straight roads, the vehicle signal amplitudes in table 3.5 are recorded.

The objective metrics lists the proxy signal measure 3.1 [1] that shows the vehicle sensitivity to crosswinds based on the lateral acceleration and the yaw velocity. In the equation 3.1, a_y is in $[m/s^2]$ and ω_z is in $[deg/s]$. The derivative of the lateral velocity 3.3 or the pure lateral acceleration and the centripetal acceleration 3.2 of the vehicle is analyzed to find the effect of the vehicle response on the subjective trigger of the driver.

Objective Metrics	
Change in lateral acceleration	Δa_y
Change in yaw velocity	$\Delta \omega_z$
Change in roll velocity	$\Delta \omega_x$
Change in steering wheel angle	Δswa
Change in steering wheel torque	$\Delta storq$
Change in proxy signal measure	$\Delta proxy$
Change in derivative of lateral velocity	$\Delta \dot{v}_y$
Change in centripetal acceleration	Δa_c
Change in lateral displacement	Δdy
Change in platform lateral acceleration	Δa_{ym}
Change in platform yaw velocity	$\Delta \omega_{zm}$
Change in platform roll velocity	$\Delta \omega_{xm}$

Table 3.5: Objective metrics of vehicle response

$$proxy = \sqrt{2a_y^2 + \omega_z^2} \quad (3.1)$$

$$a_c = \omega_z * v_x \quad (3.2)$$

$$\dot{v}_y = a_y - a_c \quad (3.3)$$

Figure 3.15 shows the OM Δa_y , which is the response to amplitude or the change from peak to peak in the response of vehicle lateral acceleration to a gust of wind. The maximum and minimum peaks are located using the ST time stamp and categorized according to the type of ST to study the driver sensitivity in terms of OM. That is, the response Δa_y that is reported to give a subjective feeling of ST2 is grouped but separated according to the test speed.

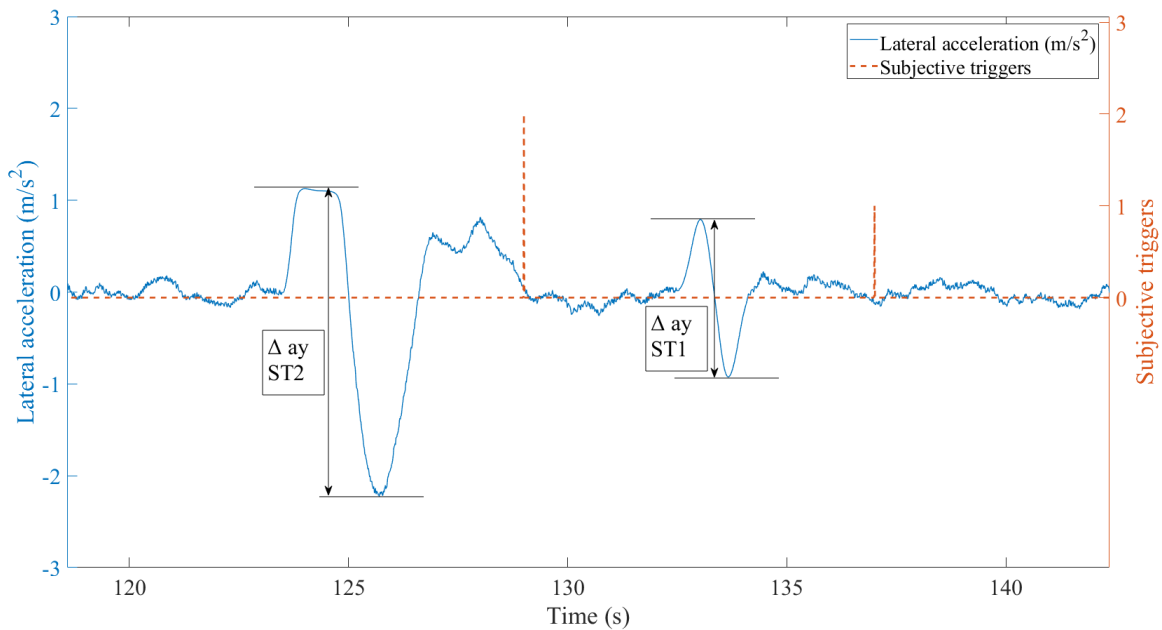


Figure 3.15: Change in vehicle lateral acceleration response

The OM vehicle responses for a common DIL simulation at 120, 160 and 200 *kph* are classified based on ST, they are presented in Appendix D.

3.10 Driving clinic and blind test

A driving clinic is organised to obtain driving data from two different group of drivers, i.e. experienced and common drivers. All 38 drivers are employees of CEVT AB, in that a group of 14 experienced drivers and amongst them 8 have experience with driving simulators. A group of 24 common drivers who are fairly new to driving and amongst them 4 have worked with driving simulator. Each driver receives an experience session before the test sessions to check if the driver is prone to motion sickness and to get used to subjective trigger reporting as explained in Section 3.8. After a driving session, the driver provides subjective feedback as shown in Section 3.7. The duration of a driving session is limited to 6 minutes and a total driving time of less than 25 minutes with breaks between is structured to provide good subjective feedback.

The driving clinic evaluates the vehicle and driver response at 120, 160 and 200 *kph*, the 3 driving sessions. Each session has 3 identical gusts of 5m/s amplitude out of 19 gusts dedicated to blind test. The purpose of this test is to filter out driving test data where the subjective trigger is not reliable and is affected by inexperience with subjective triggers. The STs of the blind test given to 1st & 9th, 9th & 19th gust are compared to evaluate the change in ST for identical 5m/s crosswind gusts of profile 1 are shown in Section 4.3 to show the effect of speed on ST.

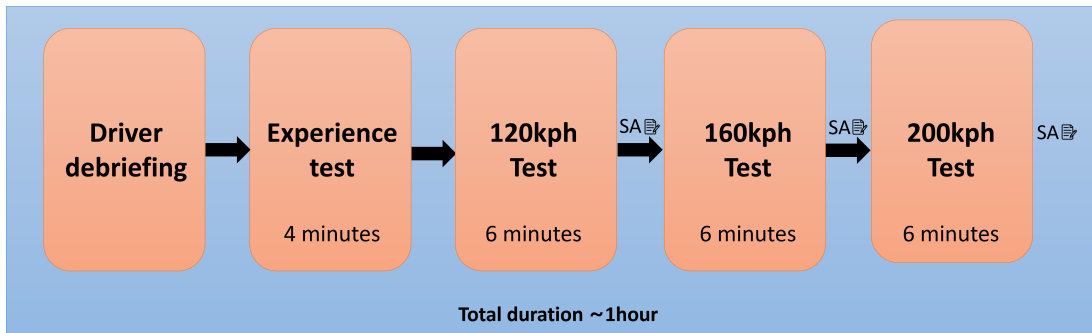


Figure 3.16: Driving clinic

3.11 Hypothesis test

The driving clinic data is used to find the correlation between the driver subjective trigger feedback and the objective metrics response of the vehicle. First hypothesis states that the ST monotonically increases with change in vehicle OM. Second hypothesis states that STs can be defined in terms of vehicle OM and the STs sensitivities do not change with vehicle speeds.

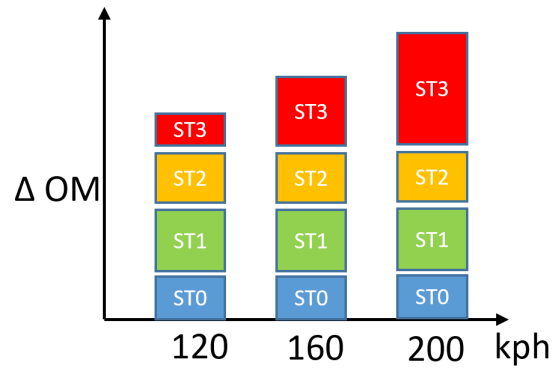


Figure 3.17: Graphical representation of the Hypotheses

The OM vehicle responses are classified based on the subjective triggers reported by driver, as shown in Figure 3.15. The first correlation hypothesis is evaluated visually on OM box plots as presented in 4.4.2 and 4.5, the first hypothesis is agreed when the increased vehicle OMs increases the severity of the driver ST.



Figure 3.18: OMs classified in terms of STs to find the relation of ST with speed

The driver ST sensitivities are defined in terms of vehicle OMs and assuming that the ST sensitivities does not change with speed, the second hypothesis test is carried to

find the relation statistically. Using One-Way ANOVA analysis to find the variation between the ΔOM at different test speeds causing the same subjective trigger as shown in Figure 3.18, the `anova1` returns a p -value for the F -statistics for the compared data samples. When the p -value greater than the 5% level of significance, the `anova-1` fails to reject the hypothesis. This means that the compared group (120, 160 200 *kph* data) means are equal for a subjective trigger.

Hypothesis statement: The vehicle responses (ΔOM) to crosswind gusts causing a subjective trigger (ST) has the equal means at different test speeds.

Reject hypothesis: When the sample data rejects the hypothesis, the ST sensitivities in terms of OMs vary with speed and shows no statistical relationship between the tested OMs at different speeds. $\mu_1 \neq \mu_2 \neq \mu_3$

Fail to reject hypothesis: When the sample data fail to reject the hypothesis, the ST sensitivities in terms of OMs does not vary with speed and shows statistical relationship between the tested OMs at different speeds.

$$\mu_1 = \mu_2 = \mu_3$$

When the `anova-1` hypothesis test fail to reject the hypothesis for an OM for all the STs, then it is a good measure to define all the ST sensitivities independent of varying test speed. When the test rejects the hypothesis it means that the OM cannot define ST sensitivity completely and is inconsistent due to varying test speed.

4

Results & Discussion

This chapter presents the vehicle and driver response to high-speed crosswind gusts at 120, 160 and 200 *kph* test speeds from the driving clinic. The subjective assessment (SA) of vehicle response and crosswind implementation is rated and is shown in Section 4.1, and the different subjective triggers (ST) at different test speeds are presented in Section 4.2. The blind test study of the driving clinic assesses the changes of drivers in subjective triggers based on test speeds, and is tabulated in Section 4.3. The null hypothesis test yields vehicle response signals that correlate with subjective triggers are presented as box plots, and the subjective trigger sensitivity in terms of objective metrics are explained in Section 4.4. Finally, the vehicle crosswind stability performance in terms of proxy signal are shown and the vehicle responses are classified based on subjective trigger in Section 4.6.

The blind test eliminated driving data that are not reliable because of a driver's varied subjective trigger sensitivity in a DIL simulation. The driving data used in the study have strictly passed the blind test, that is, a driver subjectively triggers the same response for the three identical crosswind gusts of 5 *m/s* amplitude and a duration of 1.6 seconds. The driver group percentage passing the blind test are shown below in the table 4.1.

Blind test passed	120 <i>kph</i>	160 <i>kph</i>	200 <i>kph</i>
Experienced driver %	28.5	57.1	57.1
Common driver %	16.6	45.83	45.83

Table 4.1: Percentage of drivers passing the bind test out of 14 experienced and 24 common drivers

4.1 Subjective assessment

SAs are recorded after each driving test and the tables 4.2 and 4.3 below tabulate the subjective assessment of the experienced and common driver groups at different test speeds. The SA questionnaires and the rating sheet used in the driving clinic are shown in Appendix B.1.

Subjective assessment			
Experienced drivers	120kph	160kph	200kph
Path tracking	7	6.7	5.9
Controllability	7	6.7	6
Yaw stability	6.8	6.5	5.9
Roll stability	7.3	7.1	6.3
Realistic crosswinds	7.5	7.5	7.5

Table 4.2: Subjective assessment of crosswind driving stability from experienced drivers

The SA of the experienced driver shows good and desirable implementation of crosswind gusts with a rating of 7.5, the response behavior and controllability of the vehicle shows a downward trend when the test speed increases to 200 kph. The trend is drastically reduces between 160 and 200 kph. The path tracking, controllability, yaw and roll stability SA(s) at high speed straight line driving shifts from acceptable to marginal range subjectively. The vehicle yaw stability and path tracking SA at 200 kph reports vehicle response below marginal and acceptable range.

Subjective assessment			
Common drivers	120kph	160kph	200kph
Path tracking	8	7.6	7.4
Controllability	7	7.4	7
Yaw stability	7.3	7.3	7.4
Roll stability	9	8.5	8.8
Realistic crosswinds	7.3	7	7

Table 4.3: Subjective assessment of crosswind driving stability from common drivers

The common driver SA shows varying feedback, the trend downward when test speed is increased. The crosswind gust implemented is rated an overall average of 7.1 which is a acceptable feedback. Common drivers felt that vehicle path tracking and controllability were in a good and acceptable range. The yaw and roll stability subjective feedback has not varied and also they do not show negative trend when the test speed is increased to 200 *kph*

4.2 Subjective trigger statistics

The table 4.4 shows the ST statistics for both groups of drivers. The percentage of STs occurrence vary as the test speed increases.

	Experience drivers			Common drivers		
	120 <i>kph</i>	160 <i>kph</i>	200 <i>kph</i>	120 <i>kph</i>	160 <i>kph</i>	200 <i>kph</i>
ST0 %	12.65	9.21	10.89	11.90	16.90	12.92
ST1%	56.96	54.60	43.58	52.38	40.84	38.40
ST2%	25.31	28.28	28.84	22.61	34.27	37.26
ST3%	5.06	7.89	16.66	13.09	7.98	11.40

Table 4.4: Subjective triggers statistics at different speed for two group of drivers

The ST1 occurrence percentage has reduced and the percentage of ST2 has increased when the test speed is increased in both driver groups. The experienced drivers reported an increase in ST3 and the overall trend is positively increasing along with test speed, where as common driver ST3 occurrence does not show an trend.

The ST0 percentage does not show a trend for both groups of drivers, and it is seen that the common driver average ST0 percentage is slightly higher than experienced drivers.

4.3 Blind test statistics

The tables below illustrate the relationship between vehicle speed and ST feedback for 5 m/s crosswind gust of profile 1. The driving data with identical STs as diagonal elements i.e (0,0),(1,1),(2,2) and (3,3) in the tables 4.5 to 4.10 passes the driving data through blind test filter to increase the reliability of data used to study correlation and to define ST sensitivity.

The drivers reported 39.4% ST1 and 5.26% ST2 at 120 kph speeds as shown in Tables 4.6 and 4.5, respectively, and 15.8 % ST0, that is, the drivers did not feel the gust. The table 4.8 shows an increase in both ST1 at 52.7% and ST2 at 7.9% by increasing the test speed to 160 kph . At the 200 kph test, the driver reported an increase in ST2 at 21% and a decrease in ST1 at 42.1% compared to 52.7% ST1 at 160 kph , as shown in Tables 4.9 and 4.8, respectively, and 5.26% ST0 were reported at 200 kph .

<i>Crosswind gust 1</i>	ST	0	1	2	3
	0	2.6	15.78	0	0
	1	26.31	34.21	0	0
	2	2.6	13.15	5.26	0
	3	0	0	0	0
<i>Crosswind gust 9</i>					

Table 4.5: Blind test between gust 1 and gust 9 at 120 kph

<i>Crosswind gust 9</i>	ST	0	1	2	3
	0	15.8	15.8	0	0
	1	18.42	39.4	5.26	0
	2	2.6	0	2.6	0
	3	0	0	0	0
<i>Crosswind gust 19</i>					

Table 4.6: Blind test between gust 9 and gust 19 at 120 kph

<i>Crosswind gust 1</i>	ST	0	1	2	3
	0	2.6	2.6	0	0
	1	0	15.8	23.7	0
	2	2.6	44.7	7.9	0
	3	0	2.6	0	0
<i>Crosswind gust 9</i>					

Table 4.7: Blind test between gust 1 and gust 9 at 160 kph

<i>Crosswind gust 9</i>	ST	0	1	2	3
	0	0	0	5.26	0
	1	7.9	52.7	5.26	0
	2	7.9	13.15	7.9	0
	3	0	0	0	0
<i>Crosswind gust 19</i>					

Table 4.8: Blind test between gust 9 and gust 19 at 160 kph

<i>Crosswind gust 1</i>	ST	0	1	2	3
	0	7.9	0	0	0
	1	0	34.2	34.2	0
	2	2.6	13.2	7.9	0
	3	0	0	0	0
	<i>Crosswind gust 9</i>				

Table 4.9: Blind test between gust 1 and gust 9 at 200kph

<i>Crosswind gust 9</i>	ST	0	1	2	3
	0	5.26	2.6	2.6	0
	1	0	42.1	5.26	0
	2	2.6	15.8	21	0
	3	0	0	0	0
	<i>Crosswind gust 19</i>				

Table 4.10: Blind test between gust 9 and gust 19 at 200 kph

In Tables 4.11 and 4.12, statistics show that with increasing vehicle velocity the occurrence of ST2 increases between 2.64% and 5.30% comparing 120 and 160 kph ST of the blind gust response, similarly for 160 and 200 kph an increase of 13.1% ST2 response. The occurrence of ST1 increases between 10.49% and 13.3% comparing 120 and 160 kph ST of blind gust response. But the occurrence of ST1 decreases between 10.5% and 10.6% when comparing the test data of 160 and 200 kph.

Blind test	120kph	160kph	200kph
(0,0)	2.6	2.6	7.9
(1,1)	34.21	44.7	34.2
(2,2)	5.26	7.9	7.9
(3,3)	0	0	0

Table 4.11: Percentage of ST passing the blind test comparing gusts 1 and 9 for all speeds

Blind test	120kph	160kph	200kph
(0,0)	15.8	0	5.26
(1,1)	39.4	52.7	42.1
(2,2)	2.6	7.9	21
(3,3)	0	0	0

Table 4.12: Percentage of ST passing blind test comparing gust 9 and 19 for all speeds

4.4 Hypothesis test outcome

The hypothesis test results are tabulated as shown in table 4.13, this hypothesis test is conducted on the raw data with out blind test elimination. The table 4.14 considers ST blind test elimination, the OM signal that fail to reject the hypothesis and statistically concludes the means are equal. Thus OM signals that can define ST at all speeds is a good measure to define the ST sensitivities in terms of OM. The signal passing hypothesis test is shown "1" and coloured green in the table 4.14.

OM signals that reject the hypothesis show that the OM sensitivity for an ST varies with speed and is shown as "0" in the hypothesis result table 4.13 and 4.14.

4.4.1 Null hypothesis test with all driver data

OM signals	Experienced drivers				Common drivers			
	ST0	ST1	ST2	ST3	ST0	ST1	ST2	ST3
Δa_y	0	0	0	0	0	0	0	0
$\Delta \omega_z$	1	0	0	0	0	0	0	0
$\Delta \omega_x$	1	0	0	0	0	0	0	0
Δswa	1	0	0	0	0	0	0	0
$\Delta storq$	1	0	0	0	0	0	0	0
$\Delta proxy$	0	0	0	0	0	0	0	0
$\Delta \dot{v}_y$	0	0	0	0	0	0	0	0
Δa_c	0	0	0	0	0	0	0	0
Δdy	0	0	0	0	0	0	0	0
Δa_{ym}	0	0	0	0	0	0	0	0
$\Delta \omega_{zm}$	1	0	0	0	0	0	0	0
$\Delta \omega_{xm}$	1	0	0	0	0	0	0	0

Table 4.13: Null hypothesis test outcome without blind test filter i.e considering all driver data from the driving clinic for all OMs and STs

In the table 4.13, for both the driver group most of the vehicle OM signals fail the hypothesis test. In the next section the usefulness of blind test is presented on the hypothesis test.

4.4.2 Null hypothesis test with driving data after blind test filter

OM signals	Experienced drivers				Common drivers			
	ST0	ST1	ST2	ST3	ST0	ST1	ST2	ST3
Δa_y	0	0	0	0	0	0	0	0
$\Delta \omega_z$	0	0	0	1	1	0	0	0
$\Delta \omega_x$	0	0	0	1	1	0	0	0
Δswa	1	0	0	1	1	0	0	0
$\Delta storq$	0	0	0	1	0	0	0	0
$\Delta proxy$	0	0	0	0	0	0	0	0
$\Delta \dot{v}_y$	0	0	0	0	0	0	0	0
Δa_c	0	0	0	0	0	0	0	0
Δdy	1	0	1	1	0	0	0	0
Δa_{ym}	0	0	0	0	0	0	0	0
$\Delta \omega_{zm}$	0	0	0	1	1	0	0	0
$\Delta \omega_{xm}$	0	0	0	1	1	0	0	0

Table 4.14: Null hypothesis test result from data filtered by blind test at 1 % level of significance for all OM and ST

The hypothesis results in table 4.14 is based on the data that passed blind test and it is tested at 5% level of significance.

The change in lateral displacement objective metrics defines experienced driver subjective trigger at all speeds based on the hypothesis test from anova1 for ST0, ST2 and ST3.

In the box plot shown in Figure 4.1, the smallest box plot represents the data from the 120 kph test, the widest box plot represents the data from the 200 kph test, and the middle box represents data from 160 kph.

In the box plot shown in Figure 4.2, the different speed data are combined together because they show statistical significance with each other for the same ST.

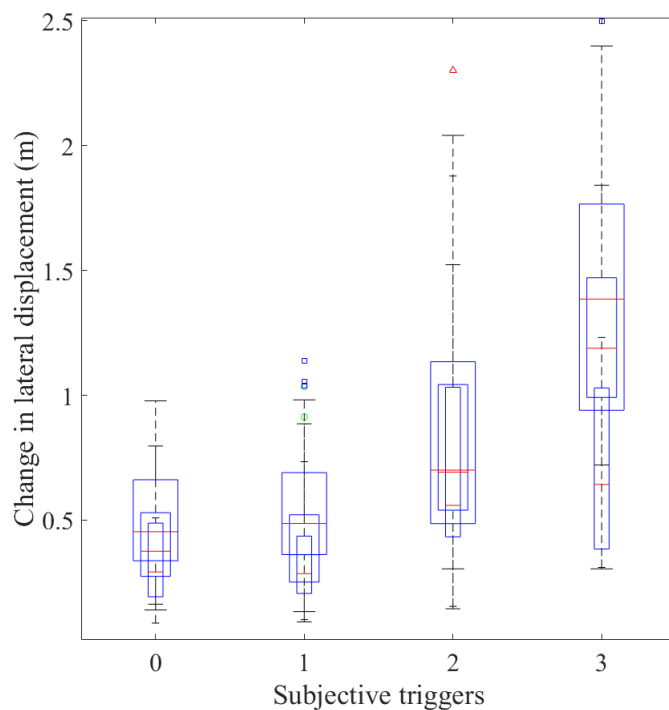


Figure 4.1: Experienced driver box plots of Δdy OM based on STs at different test speeds

The statistical distribution of data is shown as 25% lower quarterlies (LQ) and 75% upper quarterlies (UQ), the range is defined by the lower extreme (LE) and upper extreme (UE). The medians of vehicle OM correlating STs are shown in the Table 4.15 based on the box plot 4.2.

From the hypothesis test for change in lateral displacement for experienced ST1 is rejected. Thus, the sensitivity for ST1 are defined using the ST0 and ST2 as they have passed the hypothesis test statistically.

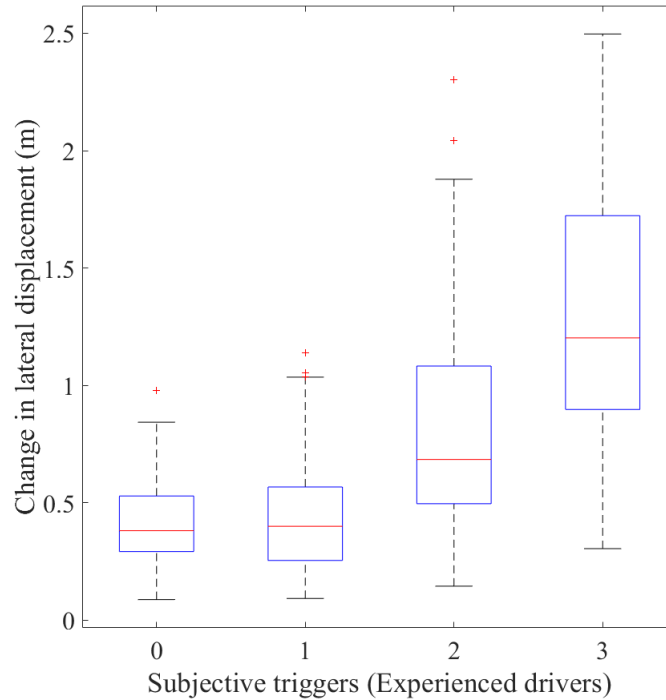


Figure 4.2: Box plot of Δdy OM correlating experienced driver STs based on hypothesis test

	OM Δdy		
	(LE,UE)	(LQ,UQ)	Median
ST0	(0.08,0.84)	(0.29,0.52)	0.38
ST1	(0.09,1.03)	(0.25,0.56)	0.39
ST2	(0.14,1.87)	(0.49,1.08)	0.68
ST3	(0.30,2.49)	(0.89,1.72)	1.20

Table 4.15: Driver ST sensitivity based on Δdy range, quartiles and median based on hypothesis test

4.5 Objective metrics rejecting hypothesis

The OM that reject hypothesis shows correlation with the both the driver ST but they vary with speed and thus cannot be used to define overall high speed straight line driving subjective trigger sensitivities.

The box plots for Δa_y of vehicle model and simulator platform are shown in figures 4.3 - 4.6.

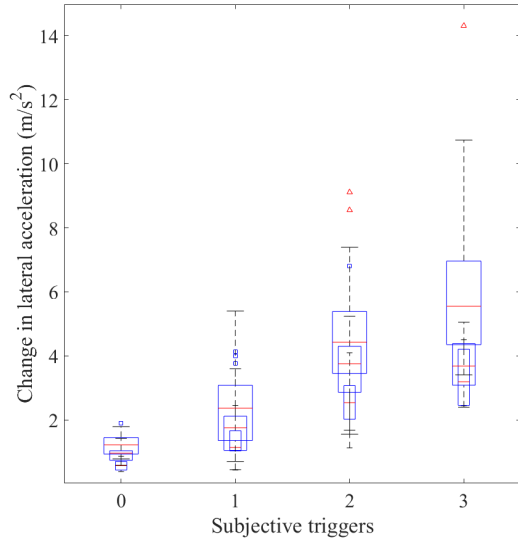


Figure 4.3: Experienced driver box plots of Δa_y OM based on STs at different test speeds

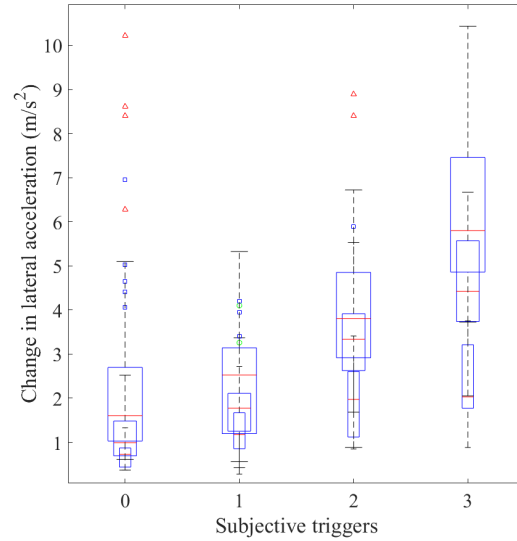


Figure 4.4: Common driver box plots of Δa_y OM based on STs at different test speeds

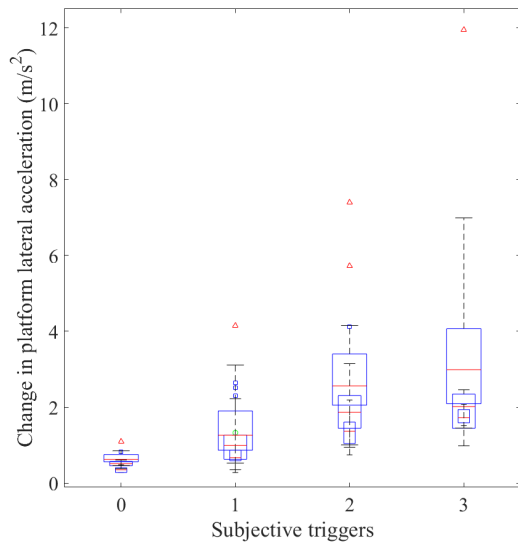


Figure 4.5: Experienced driver box plots of Δa_{ym} OM based on STs at different test speeds

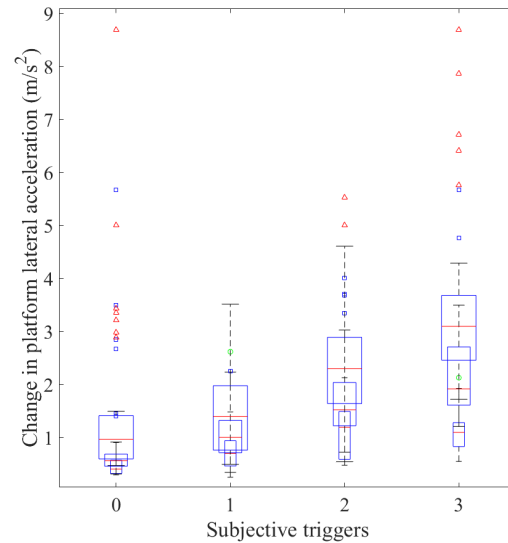


Figure 4.6: Common driver box plots of Δa_{ym} OM based on STs at different test speeds

The box plots for $\Delta\omega_z$ of vehicle model and simulator platform are shown in figures 4.7 - 4.10.

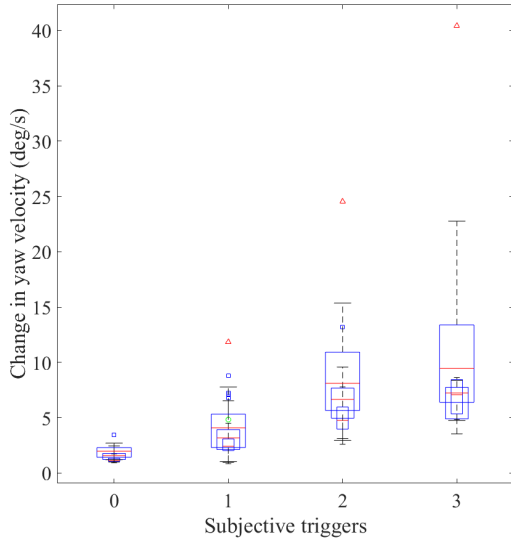


Figure 4.7: Experienced driver box plots of $\Delta\omega_z$ OM based on STs at different test speeds

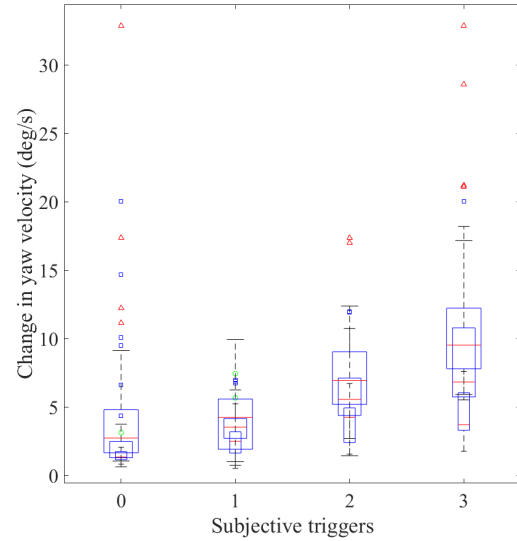


Figure 4.8: Common driver box plots of $\Delta\omega_z$ OM based on STs at different test speeds

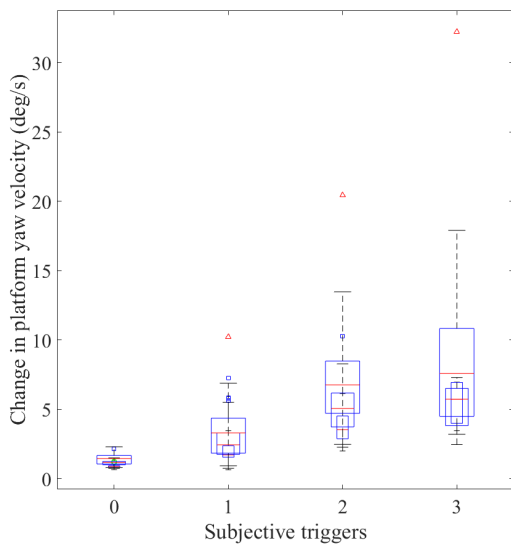


Figure 4.9: Experienced driver box plots of $\Delta\omega_{zm}$ OM based on STs at different test speeds

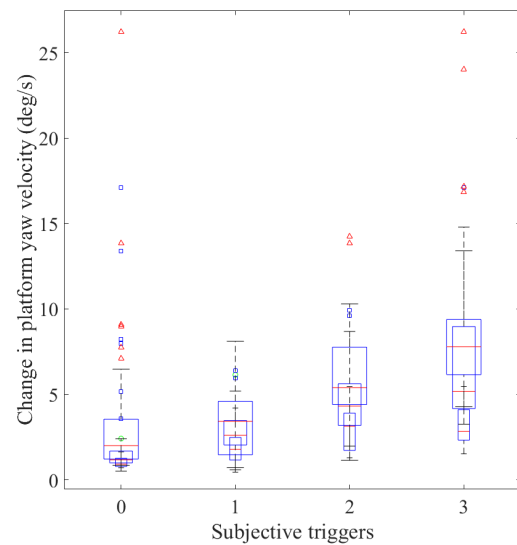


Figure 4.10: Common driver box plots of $\Delta\omega_{zm}$ OM based on STs at different test speeds

The box plots for $\Delta\omega_x$ of vehicle model and simulator platform are shown in figures 4.11 - 4.14.

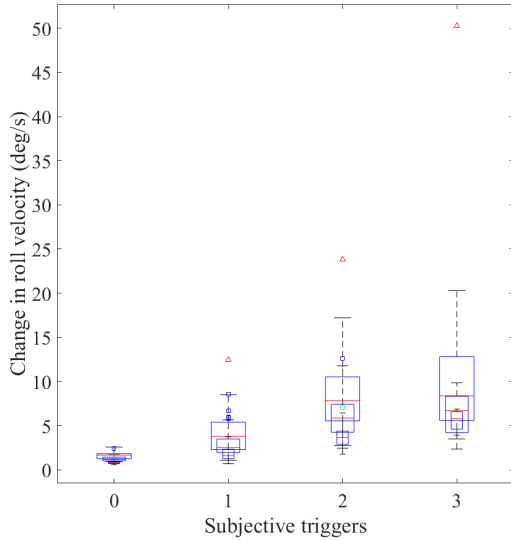


Figure 4.11: Experienced driver box plots of $\Delta\omega_x$ OM based on STs at different test speeds

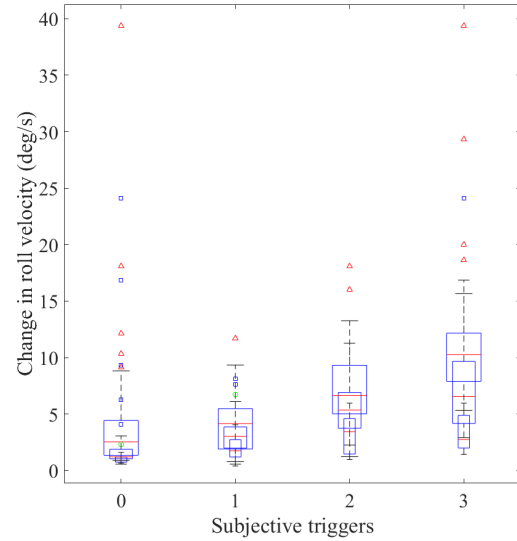


Figure 4.12: Common driver box plots of $\Delta\omega_x$ OM based on STs at different test speeds

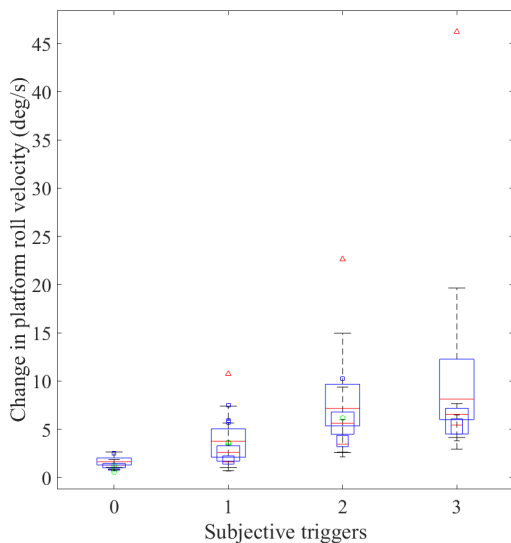


Figure 4.13: Experienced driver box plots of $\Delta\omega_{xm}$ OM based on STs at different test speeds

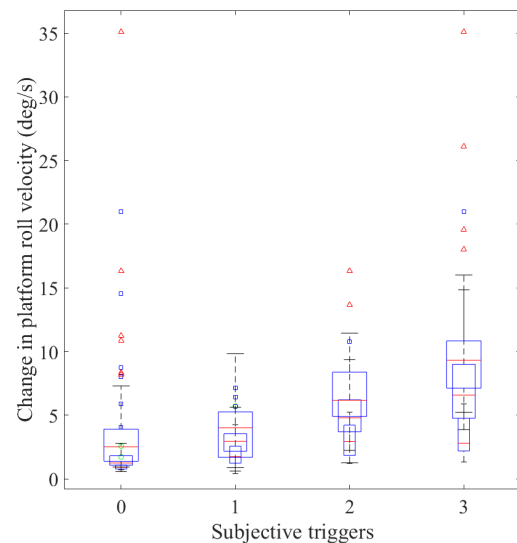


Figure 4.14: Common driver box plots of $\Delta\omega_{xm}$ OM based on STs at different test speeds

The box plots for Δa_c both the drivers are shown in figures 4.15 and 4.16.

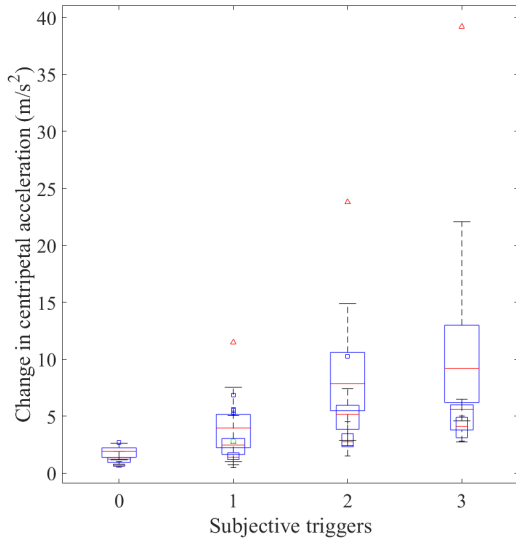


Figure 4.15: Experienced driver box plots of Δa_c OM based on STs at different test speeds

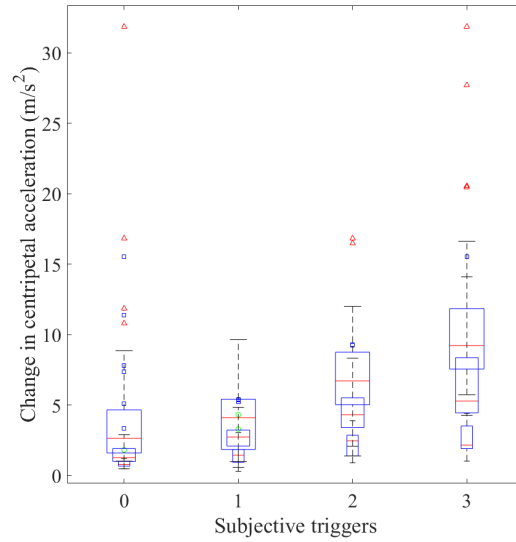


Figure 4.16: Common driver box plots of Δa_c OM based on STs at different test speeds

The box plots for Δswa by driver are shown in figures 4.17 and 4.18.

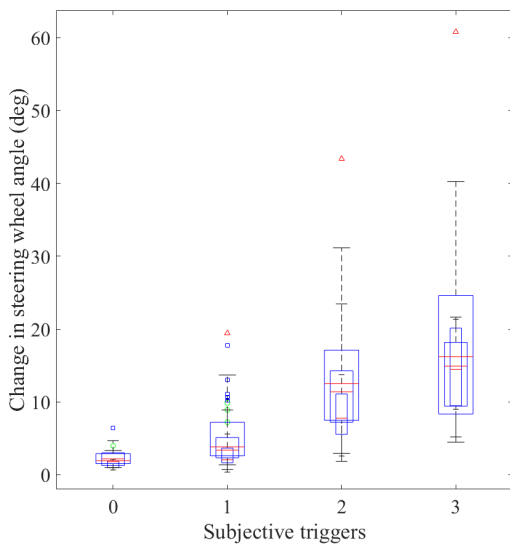


Figure 4.17: Experienced driver box plots of Δswa OM based on STs at different test speeds

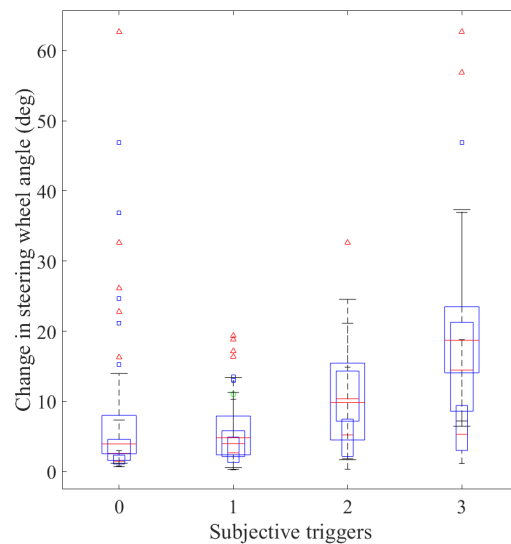


Figure 4.18: Common driver box plots of Δswa OM based on STs at different test speeds

The box plots for Δ_{storq} by driver are shown in figures 4.19 and 4.20.

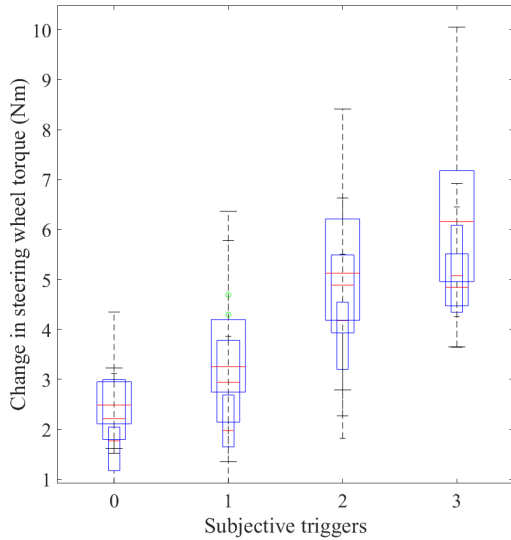


Figure 4.19: Experienced driver box plots of Δ_{storq} OM based on STs at different test speeds

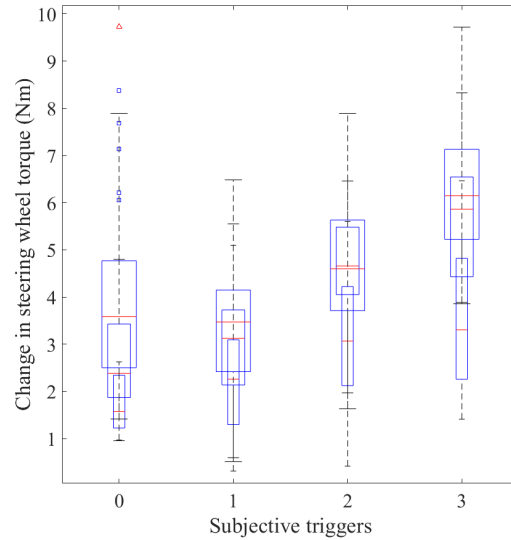


Figure 4.20: Common driver box plots of Δ_{storq} OM based on STs at different test speeds

The box plots for Δ_{proxy} by driver are shown in figures 4.21 and 4.22.

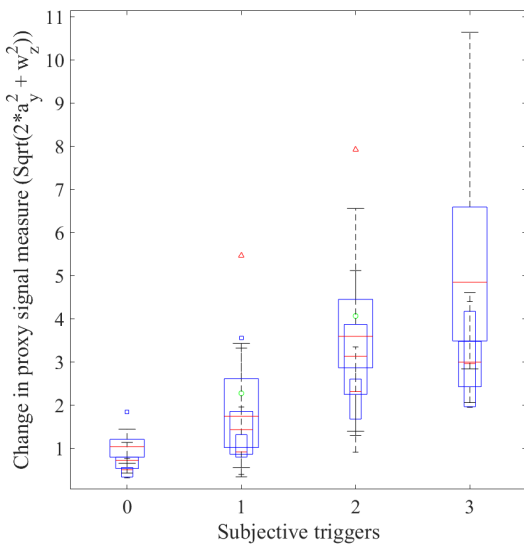


Figure 4.21: Experienced driver box plots of Δ_{proxy} OM based on STs at different test speeds

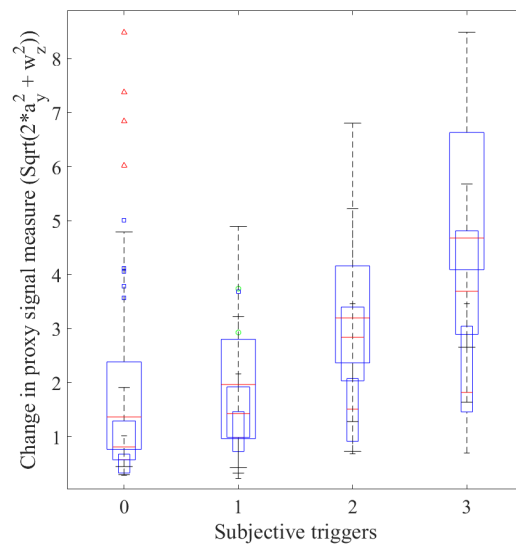


Figure 4.22: Common driver box plots of Δ_{proxy} OM based on STs at different test speeds

The box plots for $\Delta\dot{v}_y$ by driver are shown in figures 4.23 and 4.24.

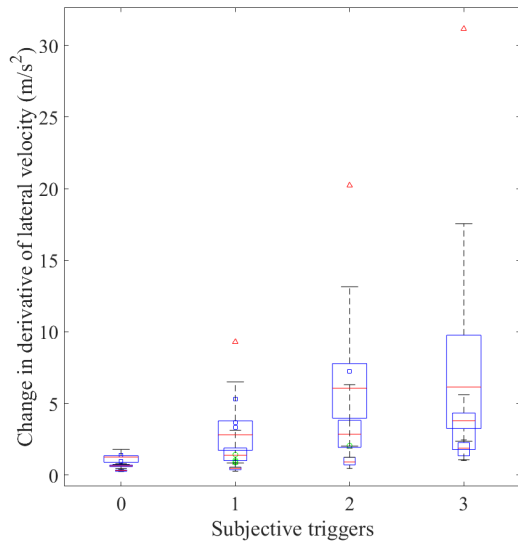


Figure 4.23: Experienced driver box plots of $\Delta\dot{v}_y$ OM based on STs at different test speeds

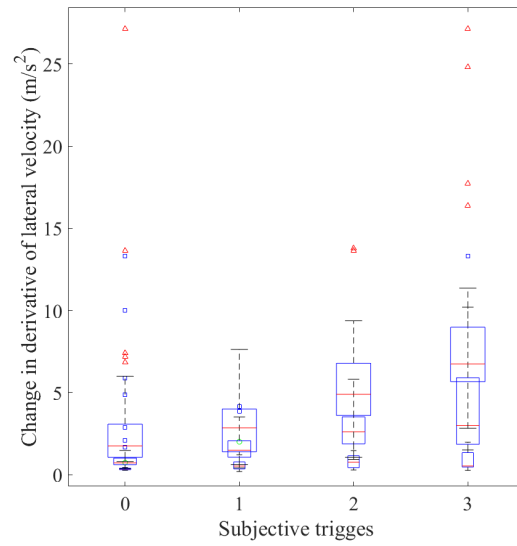


Figure 4.24: Common driver box plots of $\Delta\dot{v}_y$ OM based on STs at different test speeds

4.6 Proxy signal amplitude to evaluate overall vehicle crosswind sensitivity

The figures 4.25 and 4.26 shows experienced driver data in terms of Δa_y and $\Delta \omega_z$ vehicle response on scatter plot. The contour lines on these scatter plots are the magnitude of the change in proxy signal based on equation 3.1.

In the scatter plot, markers close to the origin show ST0 and ST1, which means that vehicle straight-path tracking was not affected and no stability issue is found. When vehicle stability in straight line tracking is affected by crosswinds, vehicle response markers move away from the origin, i.e. ST2 and ST3. Thus, the proxy measure is used evaluate the vehicle aerodynamic design performance based on the vehicle dynamic responses for the crosswind gust. Thus the increase in change in proxy moves vehicle response marker away from the origin towards instability region.

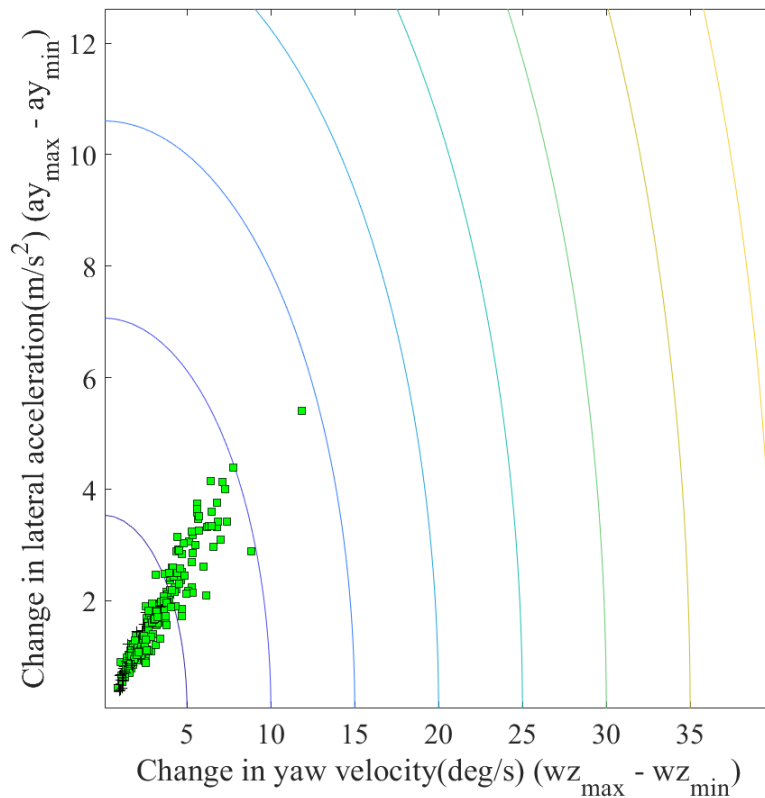


Figure 4.25: Δa_y vs $\Delta \omega_z$ scatter plot for experienced driver ST0 and ST1, $\Delta proxy$ are shown as contour lines.

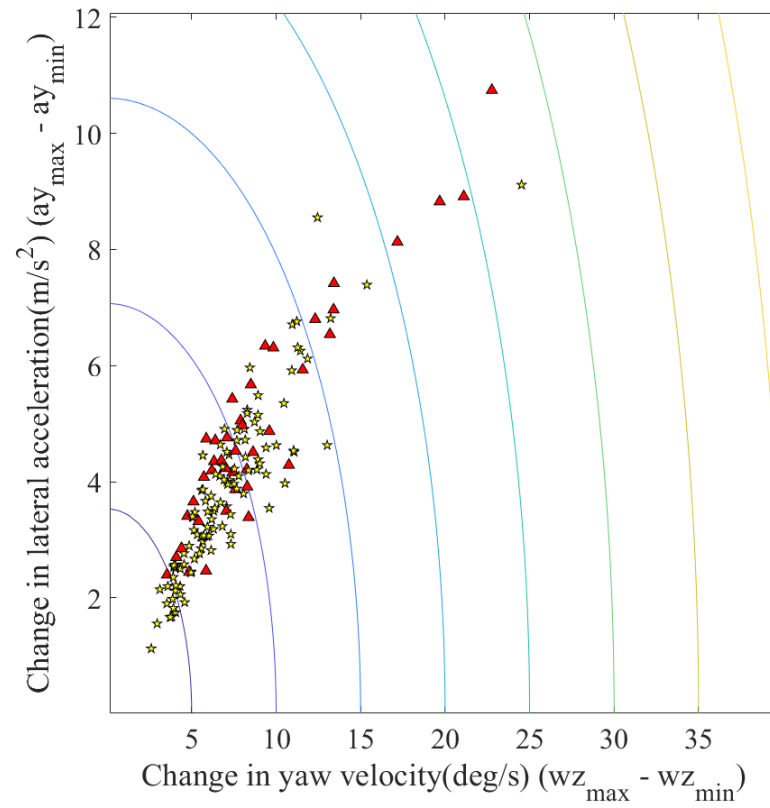


Figure 4.26: Δa_y vs $\Delta \omega_Z$ scatter plot for experienced driver ST2 and ST3, $\Delta proxy$ are shown as contour lines.

5

Conclusion

The initial focus of the study was to evaluate the complexity of the vehicle model and the coupling method. The study has configured the high-fidelity CRT vehicle model in the driving simulator to match the real-world response, and using the high-fidelity model on the CRT and the driving simulator is not affected by feedback latency. The improved two-way coupling method was essential to produce aerodynamic flow conditions that considered all types of scenario the drivers steering input caused. During the crosswind implementation the steering inputs to high-amplitude crosswinds had violent vehicle responses, and the improved two-way coupling method considers these large changes in yaw angle and body slip to give correct wind flow conditions in driver in loop simulation.

The study implemented crosswind gust in a DIL simulation of high speed driving, realistic and stochastic crosswind gusts produced the aerodynamic loads on the vehicle model that were tested in CAE simulation and in DIL simulation to setup the motion cueing. The haptic feedback of the driving simulator, the cockpit road vibration, the audio level of the vehicle environment, and the crosswind disturbances were subjectively tuned to create a DIL simulation immersive, total driving time less than 20 minutes per driver. The driving clinic study recorded 14 experienced drivers and 24 common drivers vehicle responses and subjective trigger data to find the correlation between vehicle response objective metrics and subjective feedback.

The subjective assessment shows that the implementation of crosswind gusts is good and acceptable with a rating of 7.5 to further evaluate vehicle performance based on the SA scale. The SA of vehicle performance in both driver groups points out that vehicle stability performance decreases when the test speed is increased, especially the effect of speed is seen in vehicle yaw stability and path tracking below marginal level of 5.9 rating.

The driving clinic data recorded for both group of drivers were filtered by blind test method that made the data reliable for correlating OM and driver ST. The blind test ST statistics 4.3 shows that the ST2 occurrence for crosswind gust amplitudes of $5m/s$ and profile 1 increases. The increase in subjective ST2 feedback points to the increased crosswind stability problem when the vehicle speed is increased.

The hypothesis test found vehicle lateral displacement statistically correlating with driver STs and can define ST in terms of change in lateral displacement during the tested speeds as explained in Section 3.11. When the vehicle response is stable during high speed crosswinds below $0.56 m$, i.e. ST0 and ST1 subjectively means the vehicle is stable. The subjective feeling of instability is found when change in vehicle lateral displacement is above $0.49 m$ and experienced drivers found high discomfort to control above $0.89 m$.

A proxy measure is an amplitude measure of a function based on the response of vehicle Δa_y and $\Delta \omega_z$. The scatter plot in Section 4.6 shows that when aerodynamic loads increase, the vehicle response in the plot changes away from stable driving under the crosswind gust region. Thus, the proxy measure can be used to evaluate the vehicle response to crosswind. $\Delta proxy$ correlates with the ST of the experienced driver and can be used to define the ST sensitivity of the subjective feedback of the driver.

In the real world, the occurrence of high-amplitude crosswind gusts is rare, but severely affects vehicle straight-path tracking. The degree of freedom to implement crosswind gust with high amplitudes in a DIL simulation is possible. The crosswind gusts of amplitudes between 6 to $13.5 m/s$ causes ST3 for experienced driver group and crosswind gust of amplitudes between $5.5 m/s$ to $13.5 m/s$. For common driver groups, ST3 that is defined as vehicle response is violent and vehicle control causes extreme discomfort to the driver and the Δa_y and Δa_c above $3.86 m/s^2$ and $5.44 m/s^2$ respectively induce subjective ST3 feeling in the experienced driver. For the common driver group, an excessive effort above $4.45 Nm$ to control the response of the vehicle and its trajectory in a lane demands a large $\Delta storq$ and is perceived as an uncontrolled driving scenario in high-speed driving during a gust of crosswind, giving a subjective ST3 feeling.

The box plots of vehicle OM and ST for experienced and common driver shows that common driver data has more outliers compared to experienced driver data. A general observation from subjective driving clinic evaluation shows that experienced drivers perceive roll disturbance and are more sensitive than common drivers.

5.1 Future scope

The current work is focused on implementation of crosswind gust scenario in driver-in-loop simulations for high speed straight line driving on an infinite test track with bridges and not highly detailed road side objects. Improving the virtual world with trees, building, road signs and highway exit lanes will improve the visual feedback to the driver.

The crosswind gusts implemented in this thesis are time based inputs. These crosswind gusts can be made more realistic by implementing based on distance that goes in hand

with good virtual scenario involving road side object design such as buildings, bridges, trees and other man made structures that generate crosswind gust or turbulence in the natural wind. These elements can be designed with road environment wind data to improve the driver immersion in the virtual environment and create a very close to realistic crosswinds.

The DIL simulation did not include any other road user and that caused the drivers to swerve in the lanes. The driver subjective feedback can be affected when other road vehicles are on the highway. Adding other road users will improve the DIL simulation environment and will benefit the test with subjective feedback that is similar to real world road testing but in a safe environment.

In future it will be interesting to study high-speed crosswind response on a road with large curvature or non straight line roads to study the affect in non steady state driving conditions on the driving simulator.

Bibliography

- [1] Brandt, A., J H Jacobson, B. and Sebben, S., 2022. High speed driving stability of road vehicles under crosswinds: an aerodynamic and vehicle dynamic parametric sensitivity analysis. [online] Available at: <<https://research.chalmers.se/en/publication/de9e56bc-c46a-4a1c-8601-f5a32ab77ae3>>
- [2] "Road vehicles - Sensitivity to lateral wind - Open-loop test method using wind generator input". ISO 12021:2010.
- [3] Wojciak, J. "Quantitative Analysis of Vehicle Aerodynamics during Crosswind Gusts". PhD thesis. Technical University of Munich, 2012.
- [4] Wang, L., 2021. Vehicle Dynamics Development Process With Offline and Driver-in-the-loop (DIL) Simulation. [online] Available at: <<https://odr.chalmers.se/bitstream/20.500.12380/304136/1/2021-59>>
- [5] Madhava Prakash, A., Garje Mohankumar, A., Rahul Misquith, C., Pareshe Ganatra, D., Ahmed Khan Soudagar, I. and Johnsson, J., 2021. Developing a Solution to Utilize Vehicle Dynamics Simulation Tools with a Motion Driving Simulator. [online] Available at: <<https://odr.chalmers.se/bitstream/20.500.12380/302235/1/Project>>
- [6] CEVT, 2021. VI-grade Announces Installation of DiM250 DYNAMIC Driving Simulator at CEVT. [online] Available at: <<https://newsroom.notified.com/cevt/posts/pressreleases/vi-grade-announces-installation-of-dim250-dyn>>
- [7] Brandt, A., 2021. Driving stability of passenger vehicles under crosswinds - Thesis for the Degree of Licentiate of Engineering. [online] Available at: <<https://research.chalmers.se/en/publication/521674>>
- [8] Favre, T. and Efraimsson, G. An Assessment of Detached-Eddy Simulations of Unsteady Crosswind Aerodynamics of Road Vehicles". Flow, Turbulence and Combustion 87.1 (2011), 133-163. doi: 10.1007/s10494-011-9333-4

-
- [9] DiM150 DiM250 DYNAMIC simulator | VI-grade. Retrieved 7 February 2022, from https://www.vi-grade.com/en/products/dim150_dim250_dynamic_simulator/
- [10] National WeatherService, n.d. Beaufort Wind Scale. [online] Weather.gov. Available at: <<https://www.weather.gov/mfl/beaufort>>.
- [11] (2009). Motion Cueing In The Chalmers Driving Simulator: A Model Predictive Control Approach. Retrieved from <https://publications.lib.chalmers.se/records/fulltext/98871.pdf>
- [12] Jacobson et al, B. (2007). Vehicle Dynamics Compendium. Retrieved from <https://publications.lib.chalmers.se/records/fulltext/253045/253045.pdf>
- [13] Vehicle Aerodynamics Terminology. (2010).
- [14] Jakob Huemer, Thomas Stickel, Erich Sagan, Martin Schwarz and Wolfgang A.Wall (2014) Influence of unsteady aerodynamics on driving dynamics of passenger cars, *Vehicle System Dynamics*, 52:11, 1470-1488, DOI: 10.1080/00423114.2014.944191
- [15] Kumar, A. (2021). Subjective perception and prediction model of vehicle stability under aerodynamic excitations.
- [16] AM, W., AM, F., & R, F. The impact of work practices on fatigue in long distance truck drivers. doi: 10.1016/s0001-4575(96)00044-9.
- [17] Thiffault, P. and Bergeron, J. “Monotony of road environment and driver fatigue: A simulator study”. *Accid. Anal. Prev.* 35.6 (2003), 381–391. doi: 10.1016/s0001-4575(02)00014-3
- [18] Nguyen, M. et al. “Subjective Perception and Evaluation of Driving Dynamics in the Virtual Test Drive”. *SAE International Journal of Vehicle Dynamics, Stability, and NVH* 1.2 (2017), 247–252. doi: 10.1080/00423114.2014.944191

A

Appendix 1

A.1 Vehicle response to standard crosswind gust of profile 3

The CRT vehicle and mid fidelity model lateral acceleration and yaw velocity amplitude response to crosswind gust without zero crossing with amplitude of $5m/s$ and gust duration of 1.6 seconds i.e profile 3 at 160 kph on CRT simulation are shown in the figures A.1 and A.2. The tyre normal forces are compared for close fit in figure A.3.

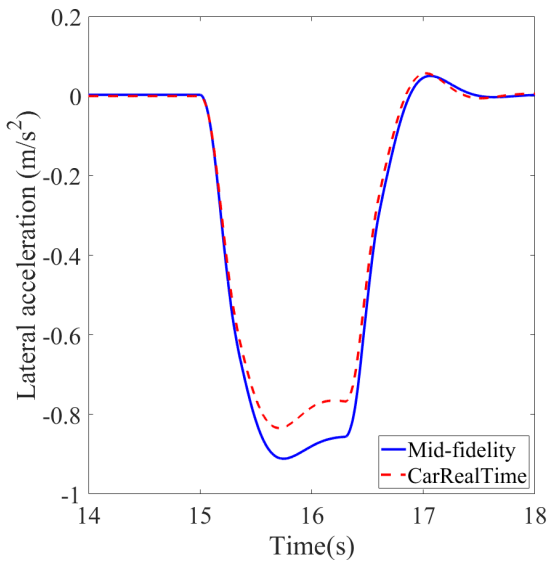


Figure A.1: Lateral acceleration amplitude response comparison between mid fidelity and CRT model

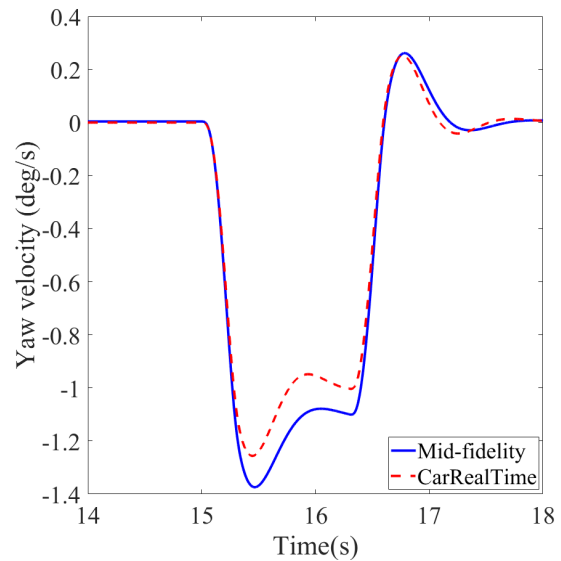


Figure A.2: Yaw velocity amplitude response comparison between mid fidelity and CRT model

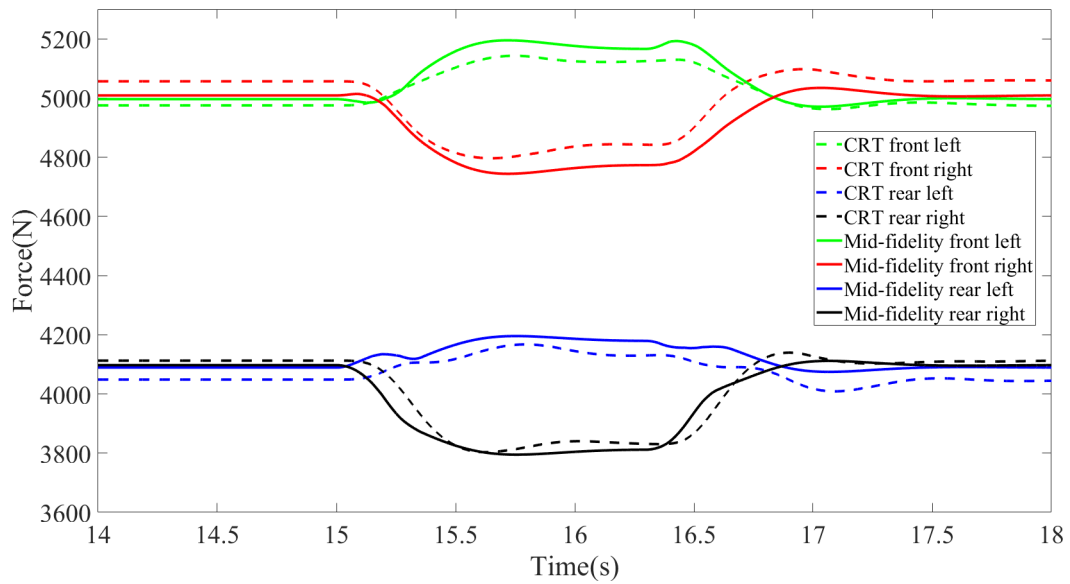


Figure A.3: Comparison of the response of normal forces of the tire between the mid-fidelity and the CRT model

B

Appendix 2

B.1 Subjective assessment and questionnaire form

Master Thesis – Driving Simulator study on crosswind aerodynamics							Week 17 and Week 18		
1	2	3	4	5	6	7	8	9	10
Worst	Too bad	Bad	Not good	Unacceptable	Marginal	Acceptable	Good	Impressive	Exceptional
<i>Subjective assessment</i>							<i>Rating</i>		
<i>Test</i>							<i>120kph</i>	<i>160kph</i>	<i>200kph</i>
<ul style="list-style-type: none"> • Path tracking How is the vehicle straight line driving? 10- The vehicle follows the straight path all time. 6- The vehicle deviates while following the straight path at times. 1- The vehicle can never follow the straight path.							<input type="checkbox"/> <input type="checkbox"/> <input type="checkbox"/> <hr/> 10	<input type="checkbox"/> <input type="checkbox"/> <input type="checkbox"/> <hr/> 10	<input type="checkbox"/> <input type="checkbox"/> <input type="checkbox"/> <hr/> 10
<ul style="list-style-type: none"> • Controllability How is the vehicle controllability during the crosswind event? 10- The driver requires no effort to control. 6- The driver requires less effort to control 1- The driver requires excessive effort to control.							<input type="checkbox"/> <input type="checkbox"/> <input type="checkbox"/> <hr/> 10	<input type="checkbox"/> <input type="checkbox"/> <input type="checkbox"/> <hr/> 10	<input type="checkbox"/> <input type="checkbox"/> <input type="checkbox"/> <hr/> 10
<ul style="list-style-type: none"> • Yaw stability How is the vehicle yaw stability during the crosswind event? 10- The vehicle yaw stability is exceptional during crosswind. 6- The vehicle yaw stability is fairly good. 1- The vehicle yaw stability is worse during crosswind.							<input type="checkbox"/> <input type="checkbox"/> <input type="checkbox"/> <hr/> 10	<input type="checkbox"/> <input type="checkbox"/> <input type="checkbox"/> <hr/> 10	<input type="checkbox"/> <input type="checkbox"/> <input type="checkbox"/> <hr/> 10
<ul style="list-style-type: none"> • Roll Stability How is the vehicle roll stability during the crosswind event? 10- The vehicle roll stability is exceptional during crosswind. 6- The vehicle roll stability is fairly good. 1- The vehicle roll stability is worse during crosswind.							<input type="checkbox"/> <input type="checkbox"/> <input type="checkbox"/> <hr/> 10	<input type="checkbox"/> <input type="checkbox"/> <input type="checkbox"/> <hr/> 10	<input type="checkbox"/> <input type="checkbox"/> <input type="checkbox"/> <hr/> 10
<ul style="list-style-type: none"> • Realistic crosswinds Is the implemented crosswinds gust event realistic? 10- The crosswinds feels the same as natural crosswinds 6- The crosswinds at times feels unnatural. 1- The crosswinds does not feel natural at all.							<input type="checkbox"/> <input type="checkbox"/> <input type="checkbox"/> <hr/> 10	<input type="checkbox"/> <input type="checkbox"/> <input type="checkbox"/> <hr/> 10	<input type="checkbox"/> <input type="checkbox"/> <input type="checkbox"/> <hr/> 10

Figure B.1: Driving clinic subjective assessment form

C

Appendix 3

C.1 Driving clinic objective vehicle signals and subjective triggers

The vehicle response signals such as lateral acceleration C.1, yaw velocity C.2, roll velocity C.3, lateral displacement C.9, proxy signal measure C.6, derivative of lateral velocity C.7, centripetal acceleration C.8 and also the driving simulator platform signal such as lateral acceleration C.10, yaw and roll velocities in figures C.11 and C.12 along with driver control response signals such as steering wheel angle C.4 and steering wheel torque demand C.5 signals are plotted with subjective triggers for each gust from an experienced driver in DIL simulation test at 160 *kph*.

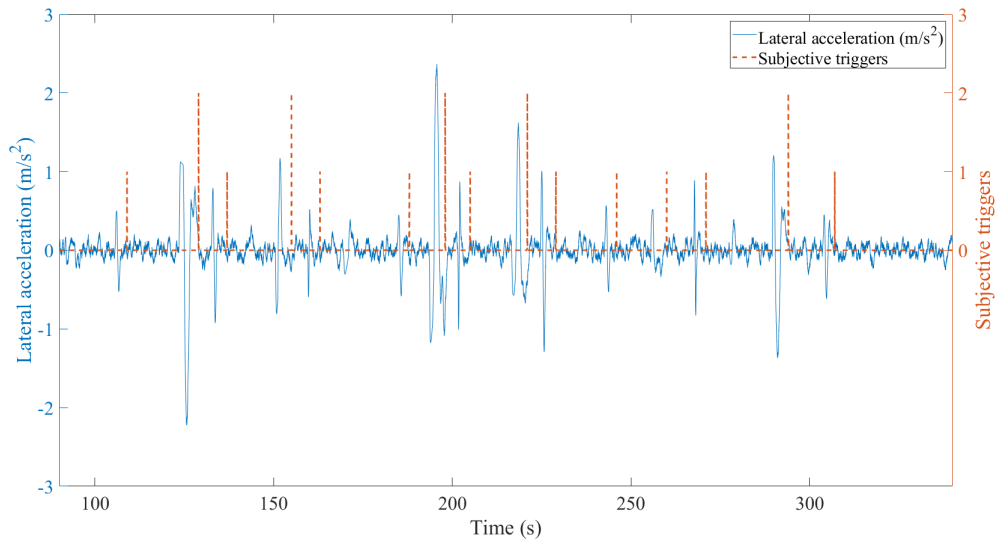


Figure C.1: a_y vehicle signal with driver ST

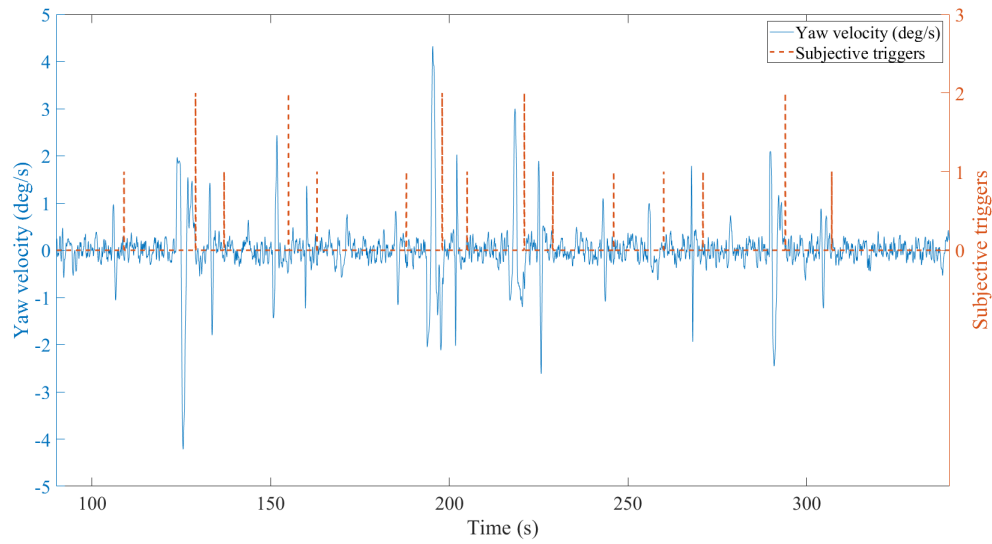


Figure C.2: ω_z vehicle signal with driver ST

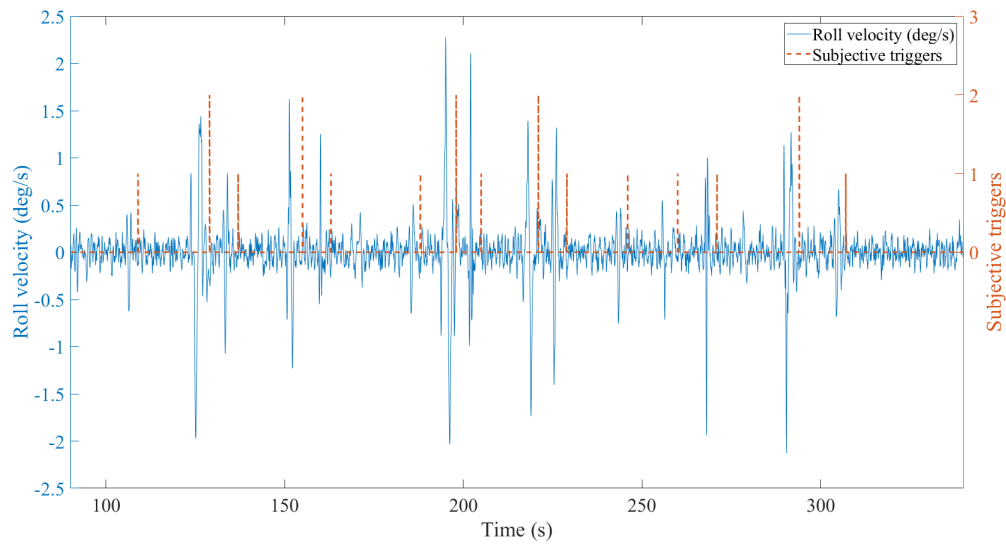


Figure C.3: ω_x vehicle signal with driver ST

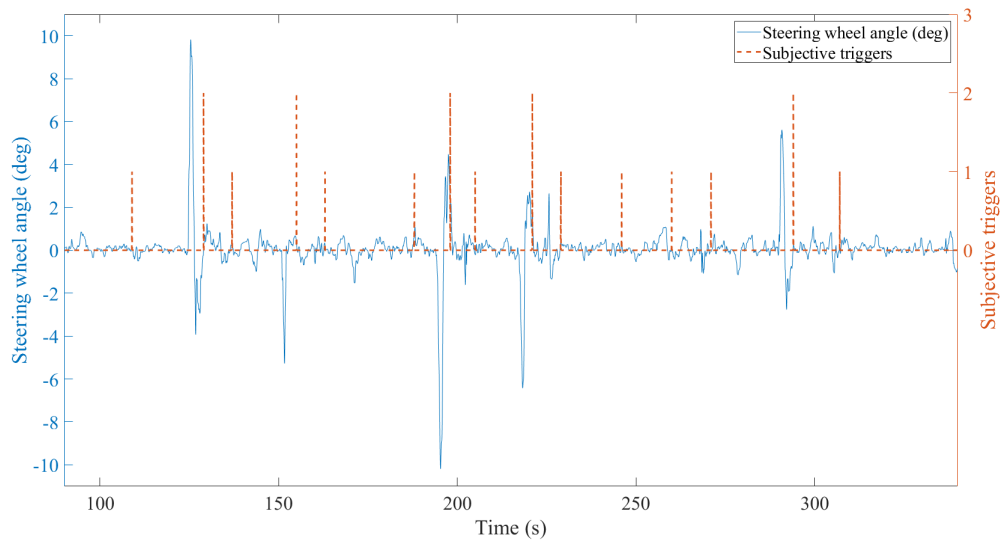


Figure C.4: *swa* vehicle signal with driver ST

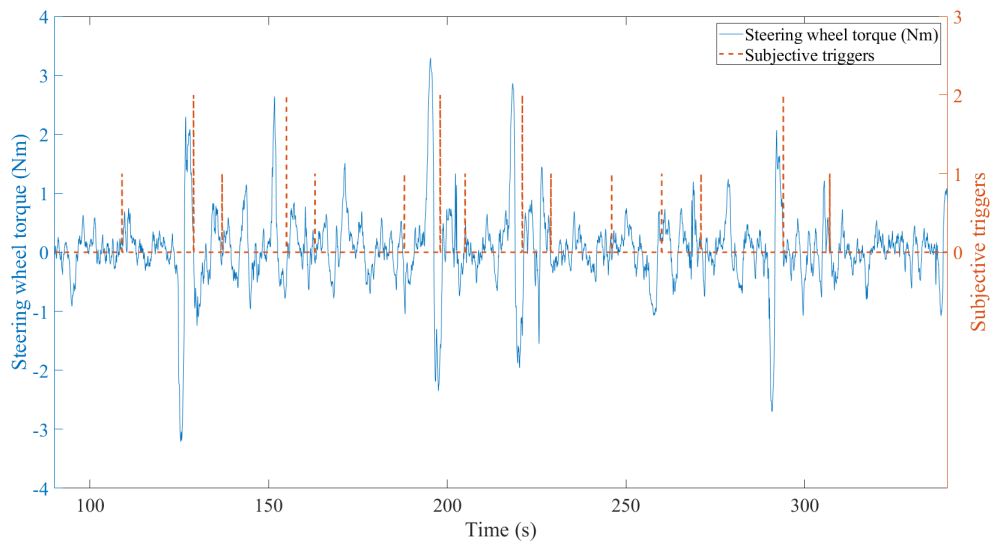


Figure C.5: *storq* vehicle signal with driver ST

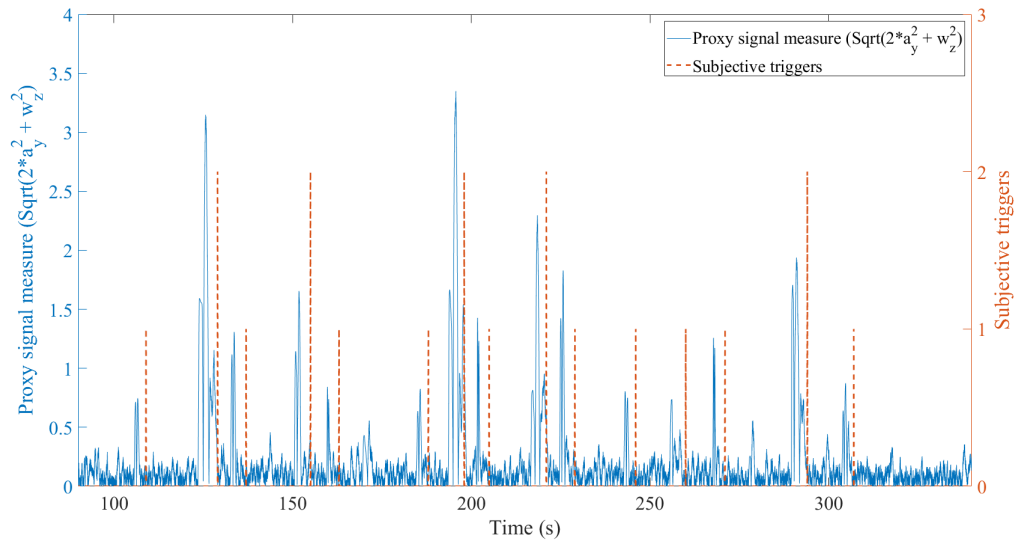


Figure C.6: *proxy* vehicle signal with driver ST

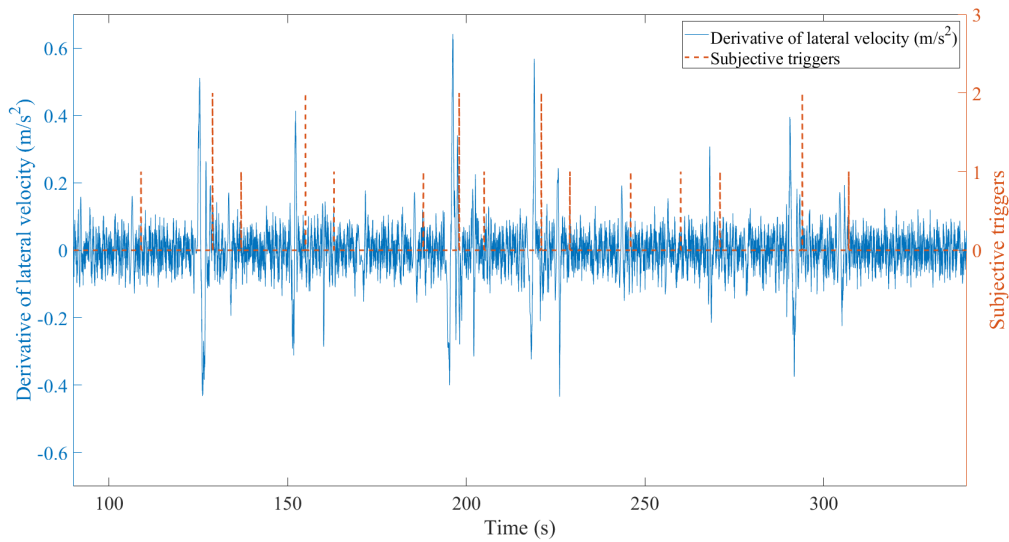


Figure C.7: v_y vehicle signal with driver ST

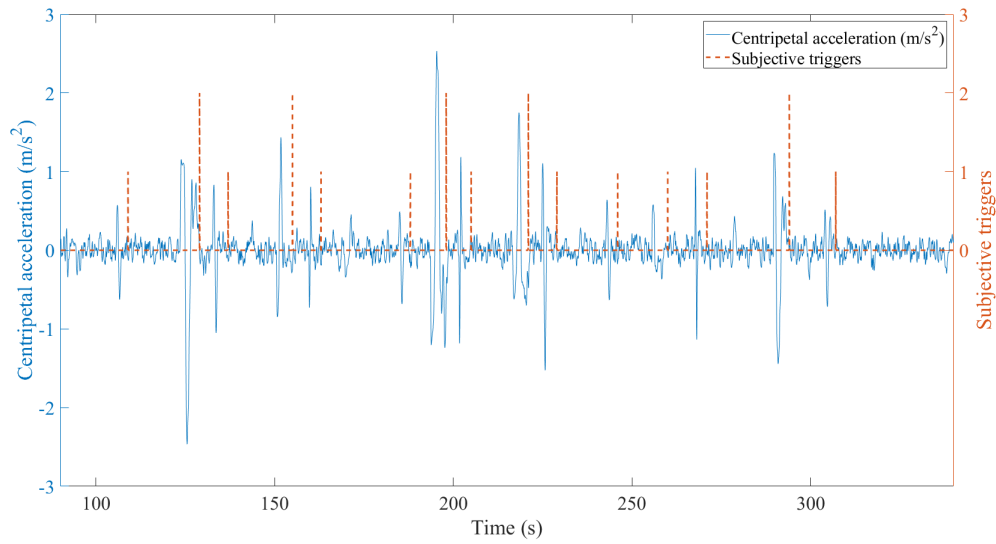


Figure C.8: a_c vehicle signal with driver ST

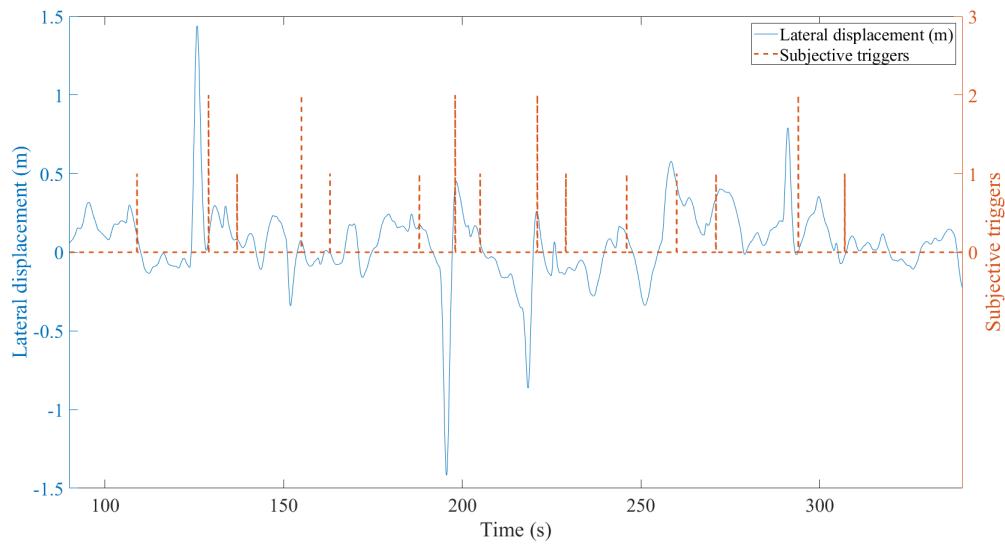


Figure C.9: dy vehicle signal with driver ST

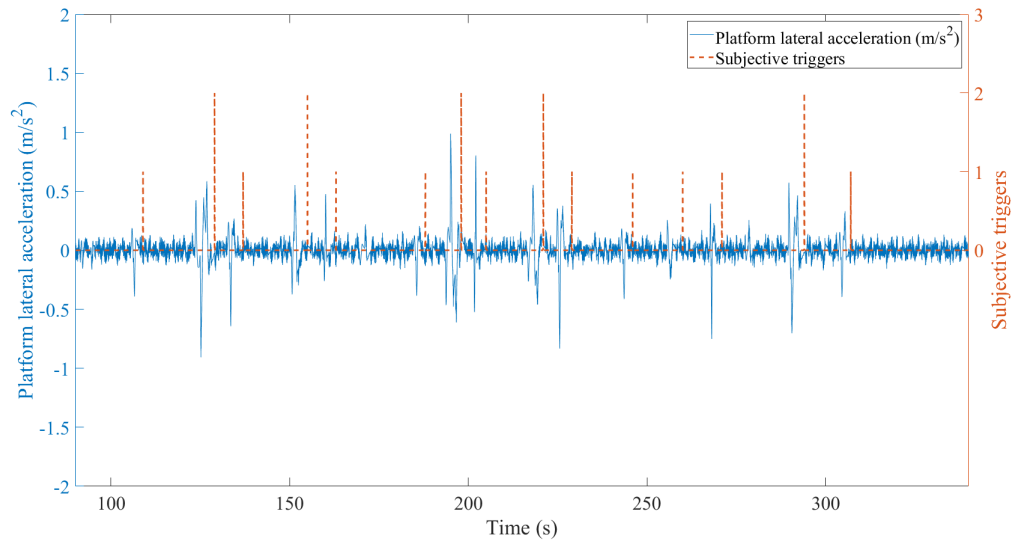


Figure C.10: a_{ym} vehicle signal with driver ST

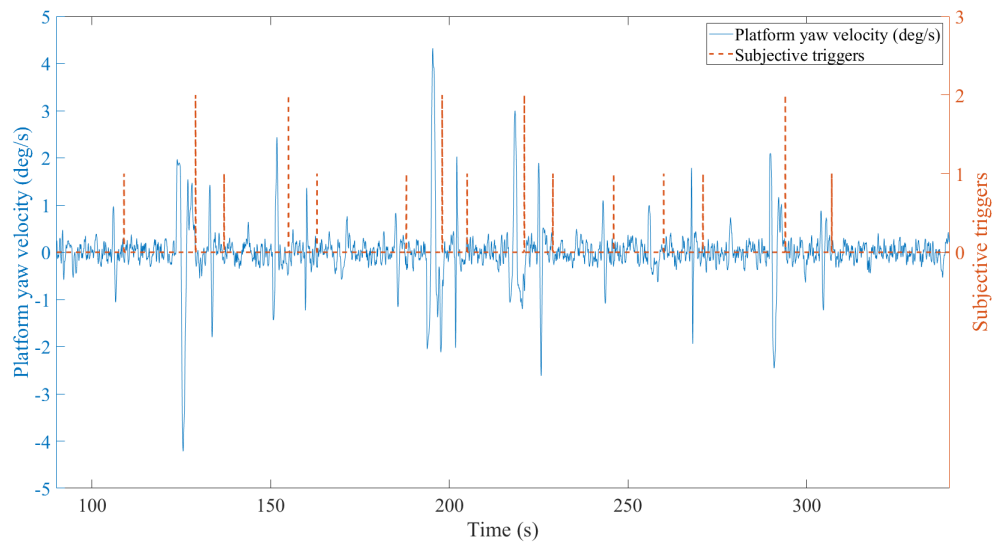


Figure C.11: ω_{zm} vehicle signal with driver ST

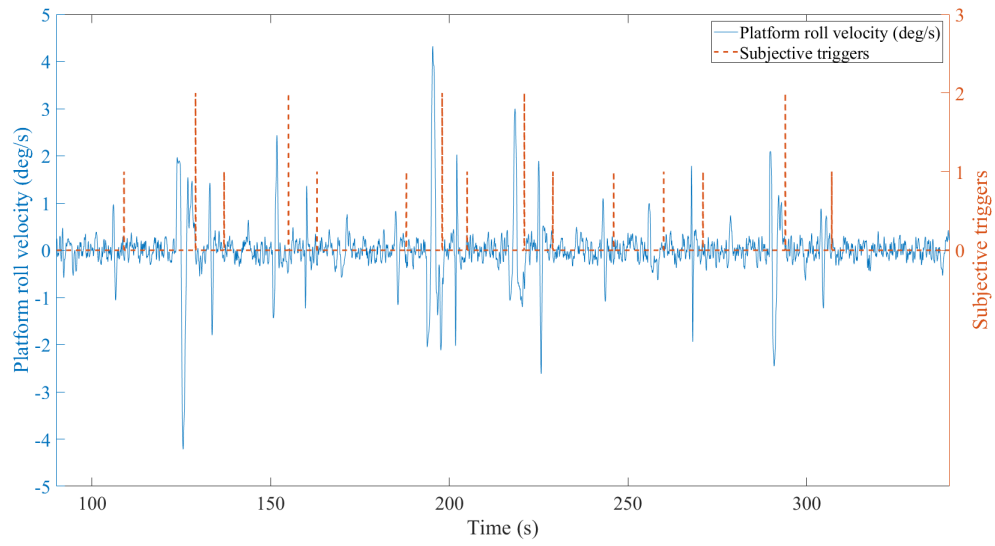


Figure C.12: ω_{xm} vehicle signal with driver ST

D

Appendix 4

D.1 Vehicle OM signal response classified by driver subjective trigger

The amplitude of vehicle OM response for crosswind gust of different amplitude are plotted and the markers or responses are classified based on the type of subjective trigger. The sections D.1.1 to D.1.3 below presents the OM and ST data from a common driver at 120, 160 and 200 *kph* test data.

D.1.1 OM and ST at 120 *kph* test

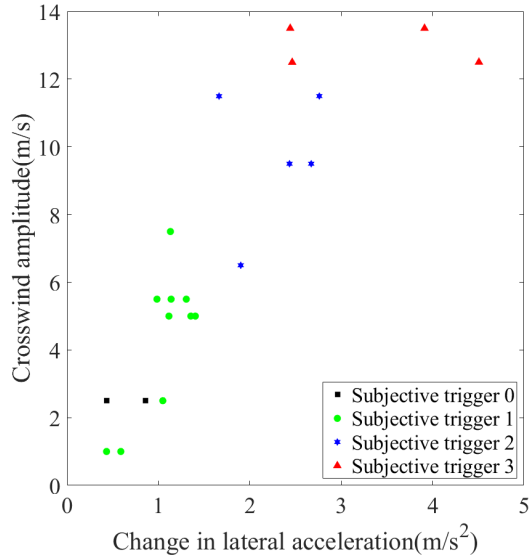


Figure D.1: Δa_y response for crosswind amplitudes grouped based on driver subjective trigger at 120 *kph*

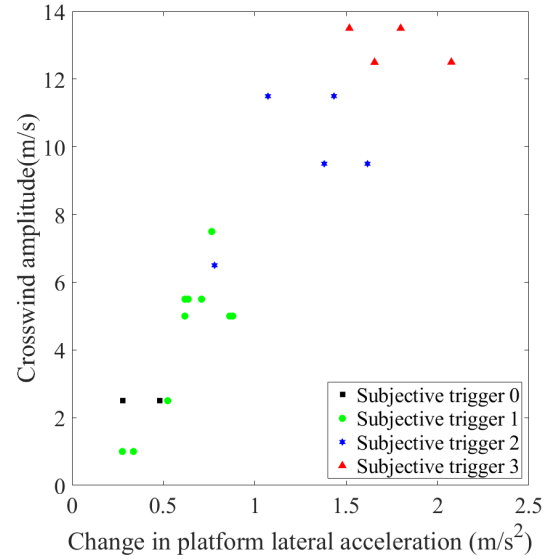


Figure D.2: Δa_{ym} response for crosswind amplitudes grouped based on driver subjective trigger at 120 *kph*

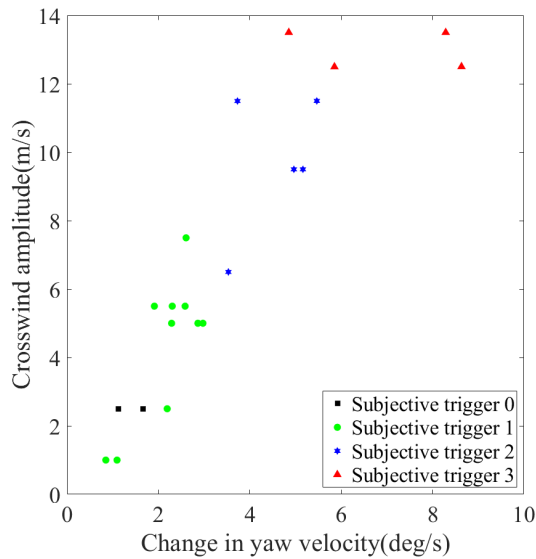


Figure D.3: $\Delta \omega_z$ response for crosswind amplitudes grouped based on driver subjective trigger at 120 *kph*

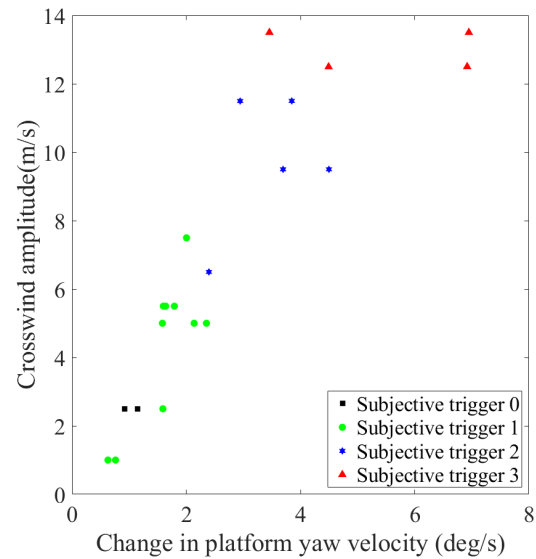


Figure D.4: $\Delta \omega_{zm}$ response for crosswind amplitudes grouped based on driver subjective trigger at 120 *kph*

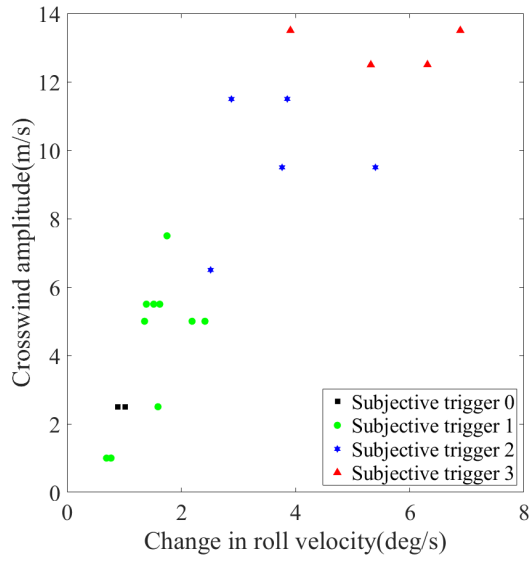


Figure D.5: $\Delta\omega_x$ response for crosswind amplitudes grouped based on driver subjective trigger at 120 *kph*

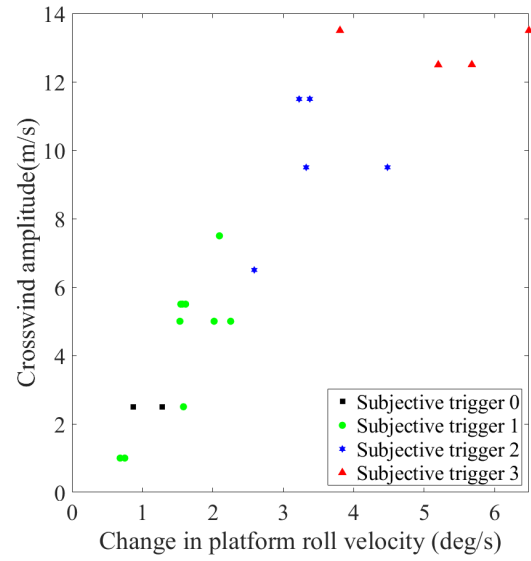


Figure D.6: $\Delta\omega_{xm}$ response for crosswind amplitudes grouped based on driver subjective trigger at 120 *kph*

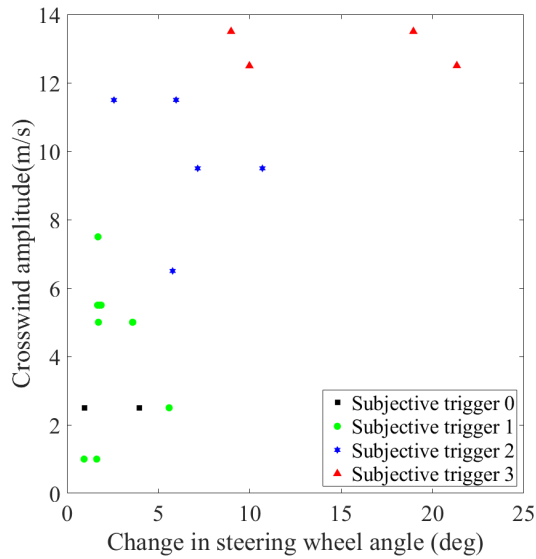


Figure D.7: Δswa response for crosswind amplitudes grouped based on driver subjective trigger at 120 *kph*

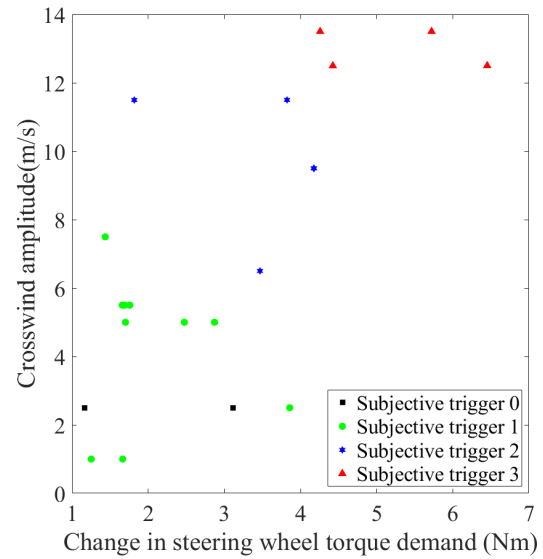


Figure D.8: $\Delta storq$ response for crosswind amplitudes grouped based on driver subjective trigger at 120 *kph*

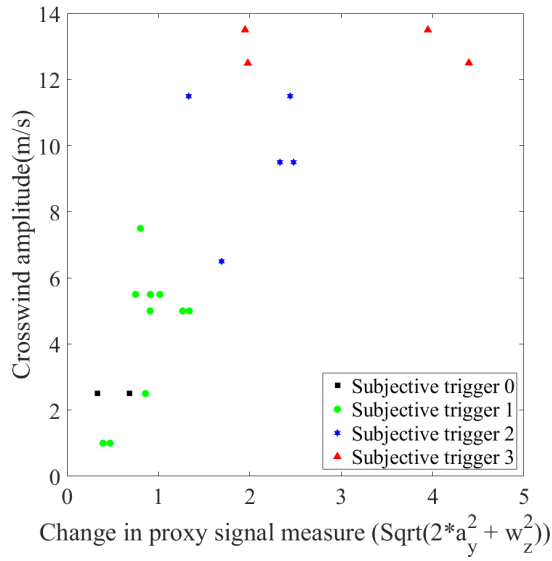


Figure D.9: Δ_{proxy} response for crosswind amplitudes grouped based on driver subjective trigger at 120 *kph*

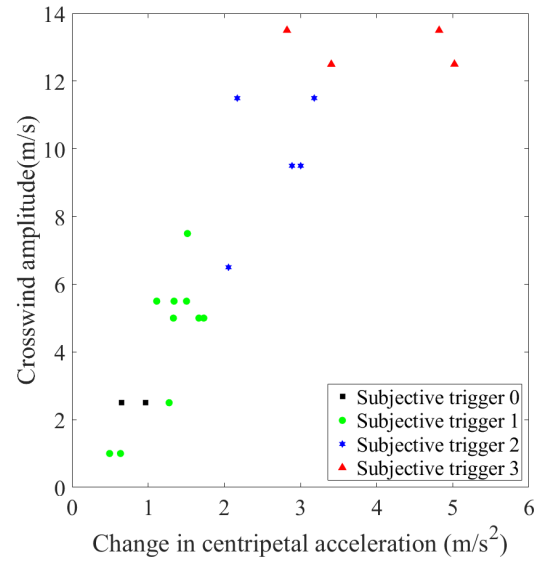


Figure D.10: Δa_c response for crosswind amplitudes grouped based on driver subjective trigger at 120 *kph*

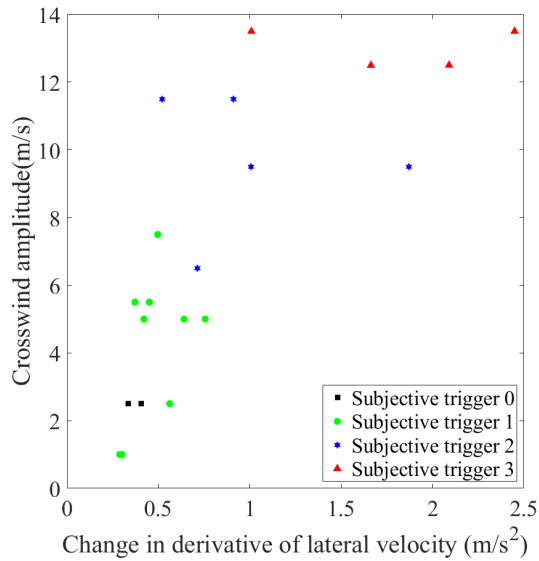


Figure D.11: $\Delta \dot{v}_y$ response for crosswind amplitudes grouped based on driver subjective trigger at 120 *kph*

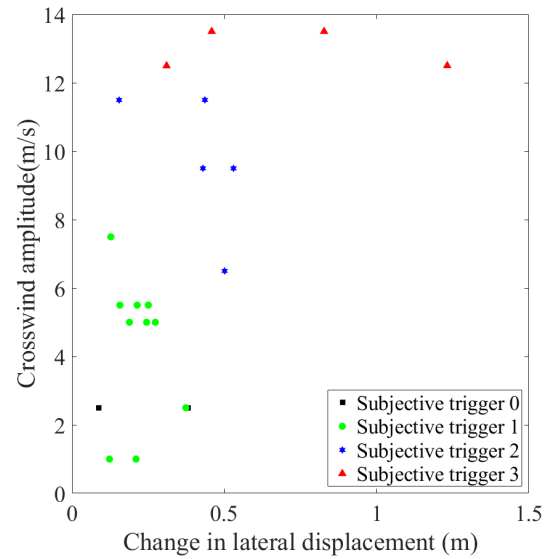


Figure D.12: Δdy response for crosswind amplitudes grouped based on driver subjective trigger at 120 *kph*

D.1.2 OM and ST at 160 kph test

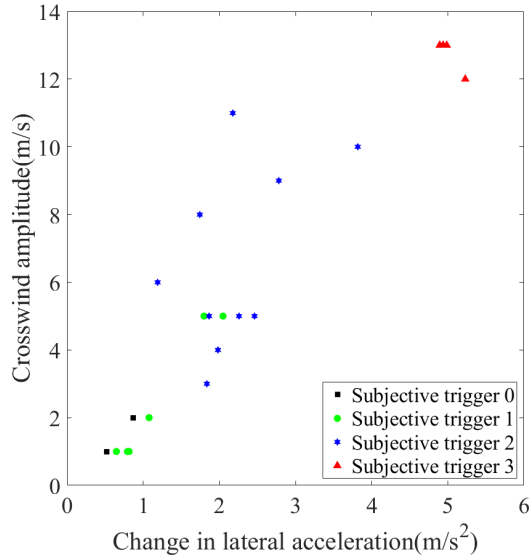


Figure D.13: Δa_y response for crosswind amplitudes grouped based on driver subjective trigger at 160 kph

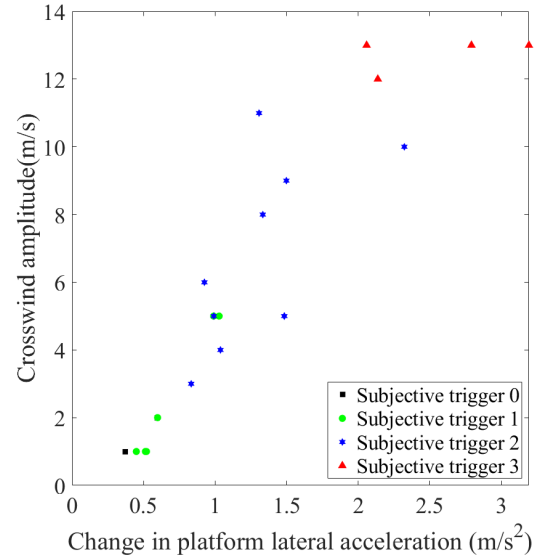


Figure D.14: Δa_{ym} response for crosswind amplitudes grouped based on driver subjective trigger at 160kph

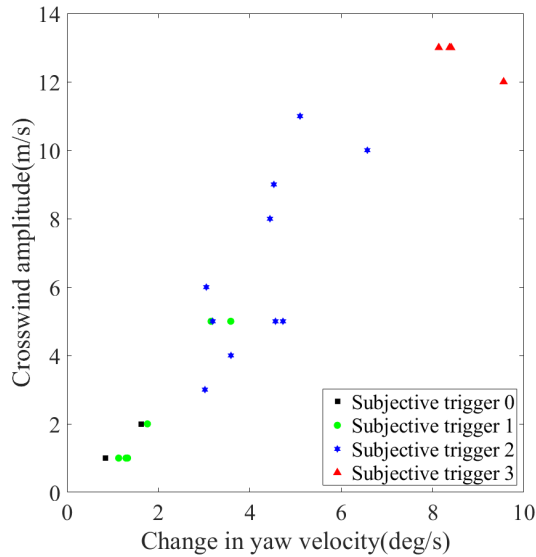


Figure D.15: $\Delta \omega_z$ response for crosswind amplitudes grouped based on driver subjective trigger at 160 kph

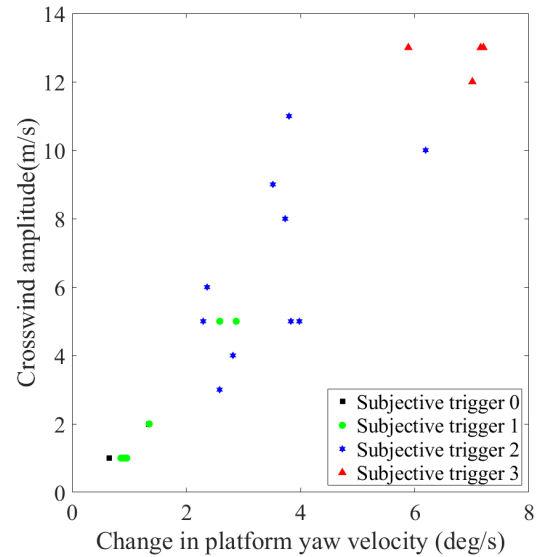


Figure D.16: $\Delta \omega_{zm}$ response for crosswind amplitudes grouped based on driver subjective trigger at 160kph

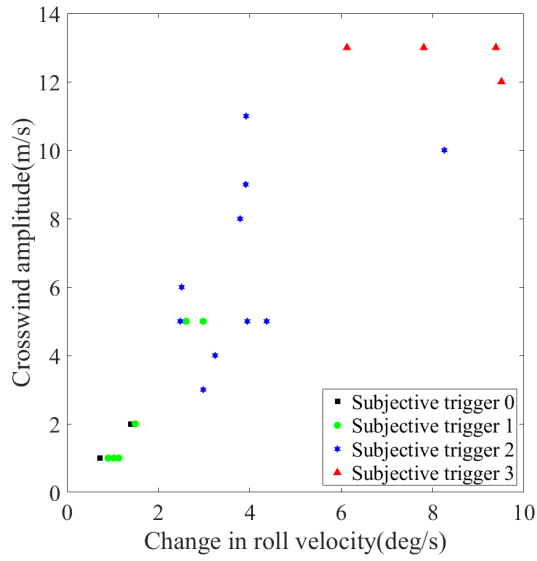


Figure D.17: $\Delta\omega_x$ response for crosswind amplitudes grouped based on driver subjective trigger at 160 *kph*

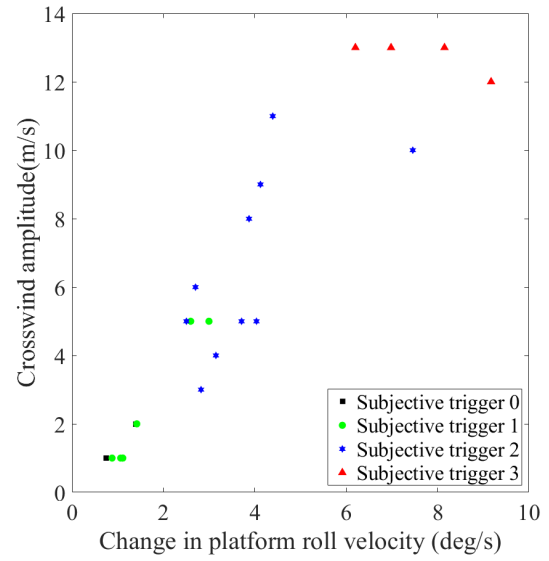


Figure D.18: $\Delta\omega_{xm}$ response for crosswind amplitudes grouped based on driver subjective trigger at 160*kph*

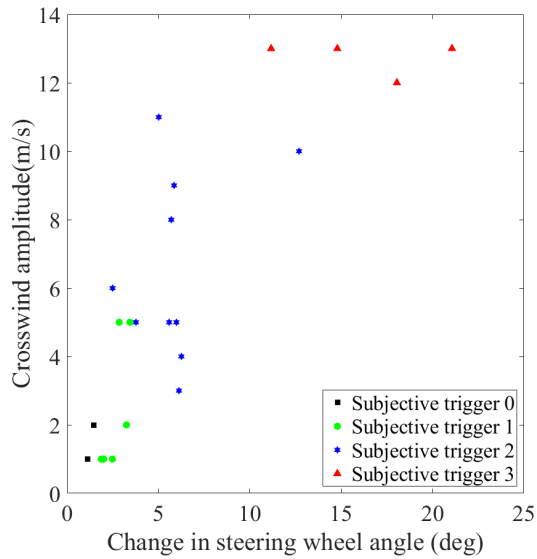


Figure D.19: Δs_{wa} response for crosswind amplitudes grouped based on driver subjective trigger at 160 *kph*

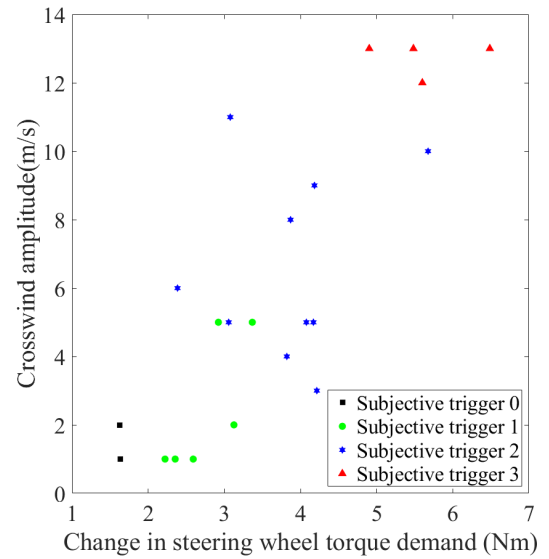


Figure D.20: Δs_{torq} response for crosswind amplitudes grouped based on driver subjective trigger at 160*kph*

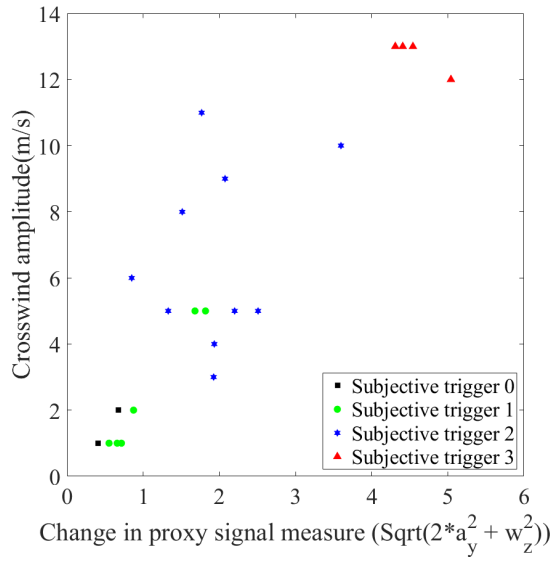


Figure D.21: $\Delta proxy$ response for crosswind amplitudes grouped based on driver subjective trigger at 160 kph

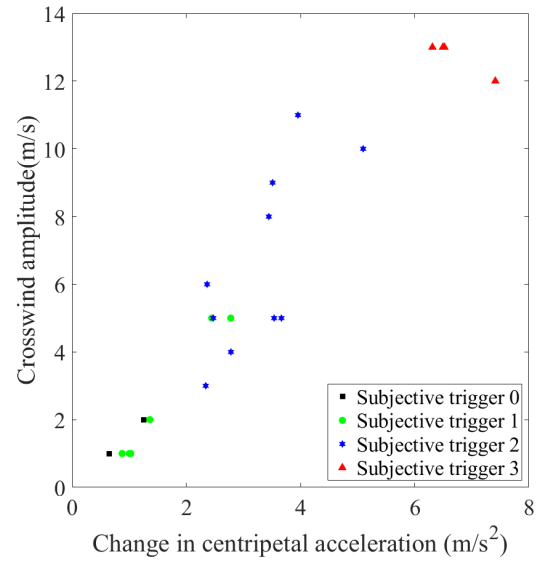


Figure D.22: Δa_c response for crosswind amplitudes grouped based on driver subjective trigger at 160kph

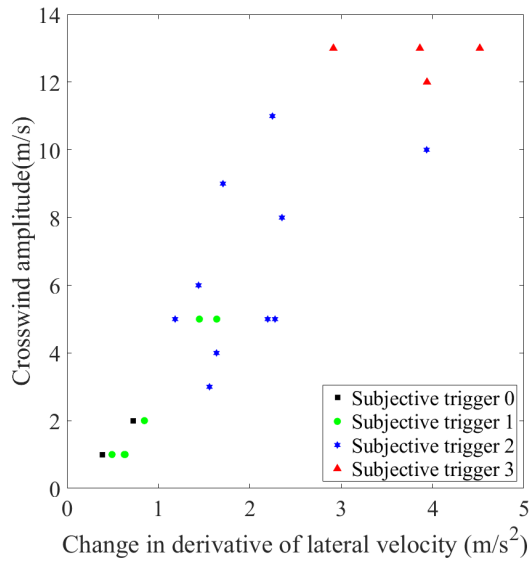


Figure D.23: $\Delta \dot{v}_y$ response for crosswind amplitudes grouped based on driver subjective trigger at 160 kph

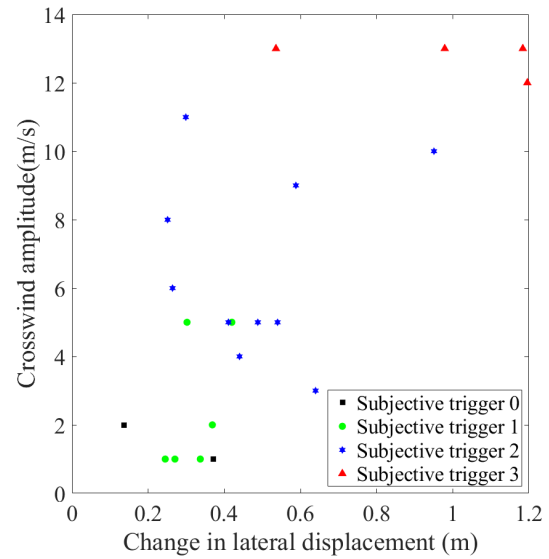


Figure D.24: Δdy response for crosswind amplitudes grouped based on driver subjective trigger at 160kph

D.1.3 OM and ST at 200 *kph* test

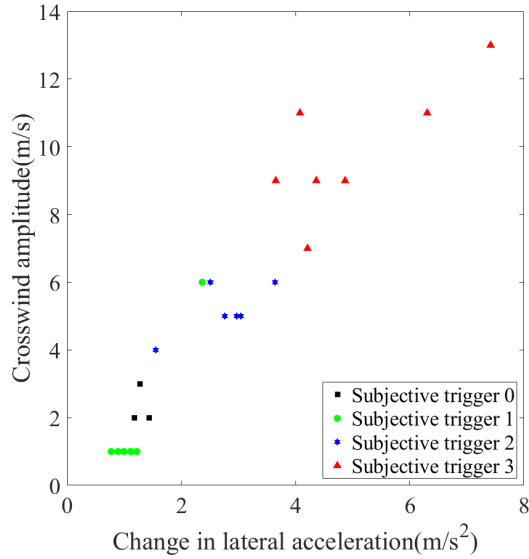


Figure D.25: Δa_y response for crosswind amplitudes grouped based on driver subjective trigger at 200 *kph*

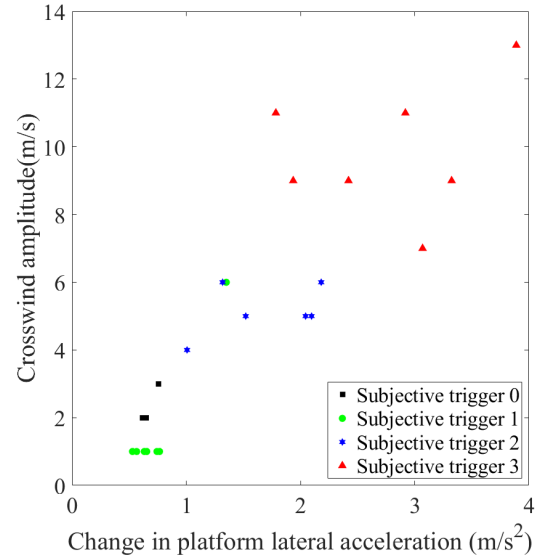


Figure D.26: Δa_{ym} response for crosswind amplitudes grouped based on driver subjective trigger at 200 *kph*

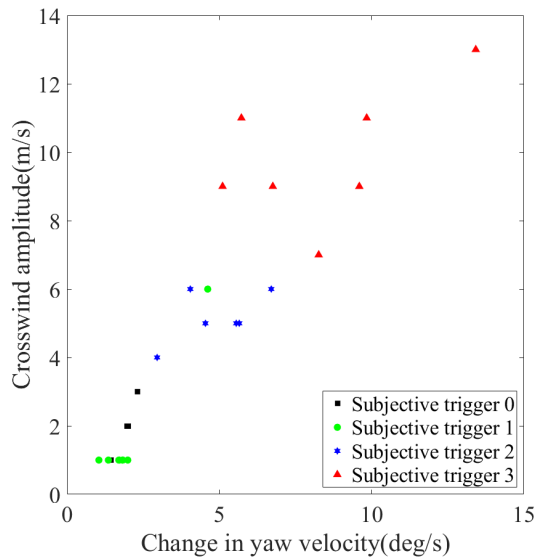


Figure D.27: $\Delta \omega_z$ response for crosswind amplitudes grouped based on driver subjective trigger at 200 *kph*

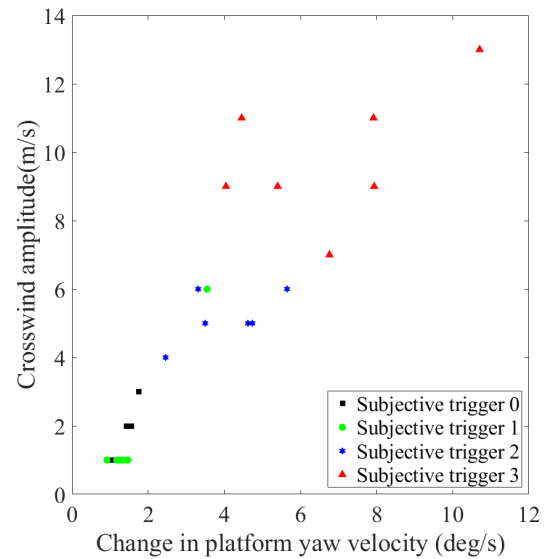


Figure D.28: $\Delta \omega_{zm}$ response for crosswind amplitudes grouped based on driver subjective trigger at 200 *kph*

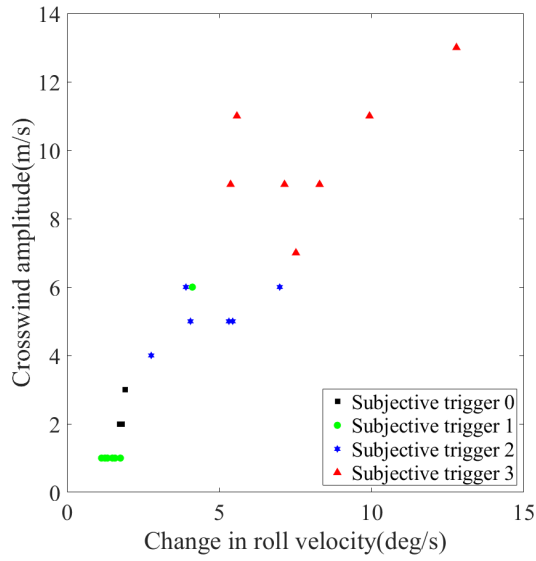


Figure D.29: $\Delta\omega_x$ response for crosswind amplitudes grouped based on driver subjective trigger at 200 *kph*

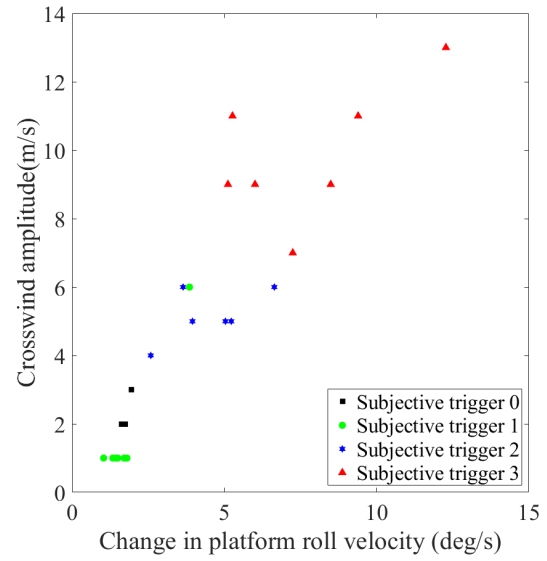


Figure D.30: $\Delta\omega_{xm}$ response for crosswind amplitudes grouped based on driver subjective trigger at 200 *kph*

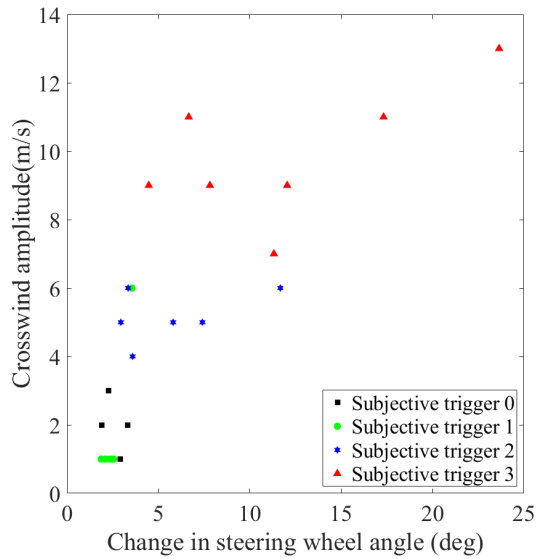


Figure D.31: Δs_{wa} response for crosswind amplitudes grouped based on driver subjective trigger at 200 *kph*

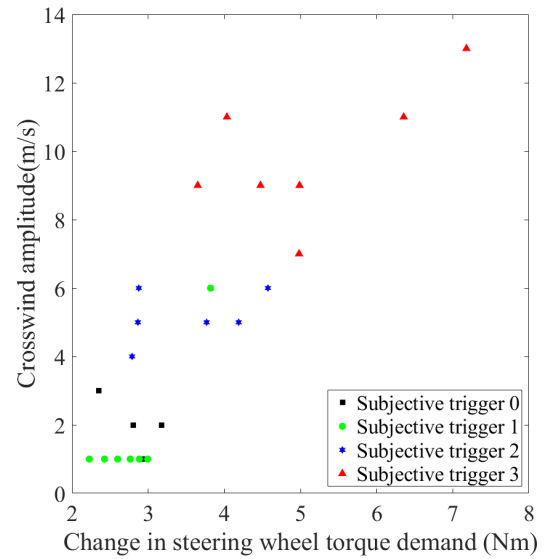


Figure D.32: Δs_{torq} response for crosswind amplitudes grouped based on driver subjective trigger at 200 *kph*

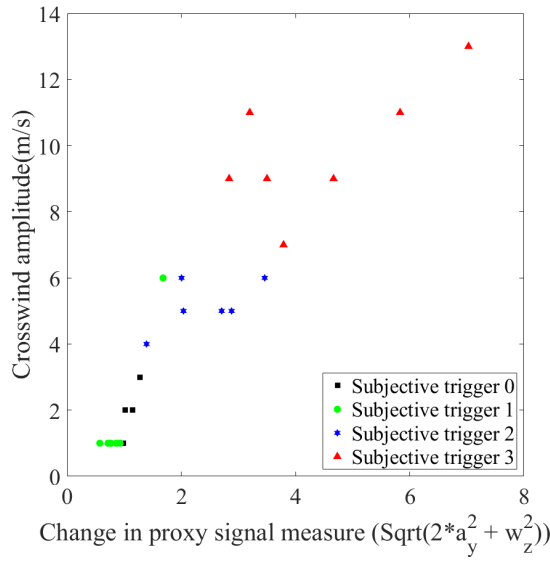


Figure D.33: Δ_{proxy} response for crosswind amplitudes grouped based on driver subjective trigger at 200 *kph*

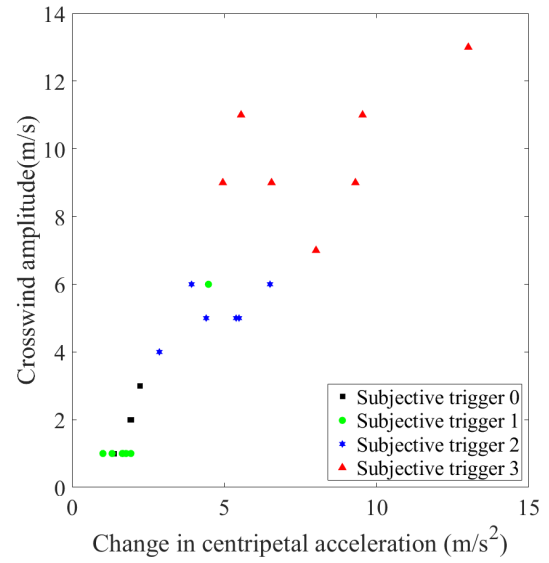


Figure D.34: Δ_{a_c} response for crosswind amplitudes grouped based on driver subjective trigger at 200 *kph*

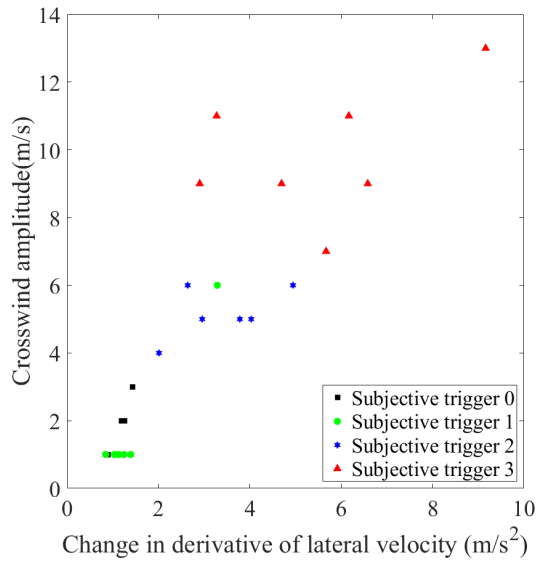


Figure D.35: $\Delta_{\dot{v}_y}$ response for crosswind amplitudes grouped based on driver subjective trigger at 200 *kph*

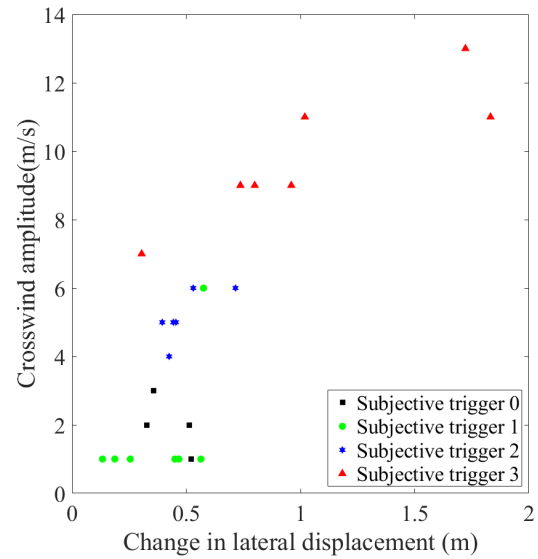


Figure D.36: Δ_{dy} response for crosswind amplitudes grouped based on driver subjective trigger at 200 *kph*

DEPARTMENT OF SOME SUBJECT OR TECHNOLOGY
CHALMERS UNIVERSITY OF TECHNOLOGY

Gothenburg, Sweden
www.chalmers.se



CHALMERS
UNIVERSITY OF TECHNOLOGY